University of L'Aquila
Istituto Italiano di Tecnologia

Department of Engineering
Master's Thesis

Coding and decoding in a neuro–robotic closed loop system: Connecting neurons and artificial devices

Advisor
Dr. Pierdomenico Pepe

Co-Advisor
Dr. Michela Chiappalone

Candidate
Sreedhar Saseendran Kumar

Erasmus Mundus Masters Course
in
Mathematical Modelling in Engineering (MATHMODS)
Academic cycle 2010-'12

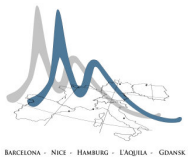

Acknowledgements

This thesis work would not have been possible without the guidance and the help of several individuals who in one way or another contributed and extended their valuable assistance in the preparation and completion of this study.

I wish to thank Dr. Michela Chiappalone, for her unselfish and unfailing support as my thesis adviser for making me feel at ease with a new branch of study, and the gentle introduction to neuroscience.

Jacopo Tessadori for his patience, encouragement, valuable insights into topics of relevance, and productive discussions on a variety of topics. I am grateful to him for always being available; whether to clarify a doubt or discuss a concern.

Prof. Pierdomenico Pepe, for readily agreeing to act as my academic advisor, for his concern regarding my work, and his valuable suggestions.

Prof. Bruno Rubino, our course co-ordinator who was very supportive of my efforts to find a thesis project in an area of study of my choice.

Rouhullah Habibie, friend and room-mate, for the long and enthusiastic discussions on topics ranging from perspectives in neuroscience, the scientific method to religion and philosophy.

My colleagues and staff at the Istituto Italiano di Tecnologia, for making my brief stay in Genoa, an experience to cherish for a long time.

Divya.S. Gopan, for her rock solid support whenever I needed it the most.

My family, friends and well wishers for the strength and encouragement.

-Sreedhar Saseendran Kumar

Abstract

An experimental setup capable of real-time closed-loop experiments on *in-vitro* neural networks is a powerful tool for the investigation of information processing in the central nervous system, since it provides a straightforward mean to evaluate hypotheses on coding and decoding schemes. Such a system was designed, implemented and tested at the Istituto Italiano di Tecnologia, with some degree of success: a small robot moves in an arena containing obstacles, collecting information on its environment through proximity sensors. Such information is coded to a dissociated neural culture and recorded signals are in turn decoded and used to drive the robot in an obstacle avoidance task.

However, control of the robot has so far been limited. Though closed-loop experiments showed a significant increase of traveled path between hits, control of the robot was still fairly limited: while a preference to turn in a direction rather than another can be conveyed, fine control of wheel speeds was still out of reach. One of the main reasons for this partial failure could be the fact that the coding and decoding strategies implemented were too simple to properly "translate" information: both schemes relied on a simple, linear, frequency-based relation. Especially in the decoding case, several other signal features must be taken into account, such as organization of spikes into bursts, order of firing and delay between events.

In this thesis project, the organization of spikes into bursts has been taken up in particular. Appropriate software modules were developed to this end. The algorithms were tested on an offline test-bed, and the results verified before they were integrated into the modular architecture of the existing custom software, written in C#. The impact of the augmented scheme was tested using closed-loop neuro-robotic experiments, in order to evaluate the actual performance of the proposed decoding scheme with living networks.

The results of the experiments are presented. In the current form, the augmented decoding scheme does not seem to be contributing significantly to the performance of the robot. This could be due to a variety of reasons. A discussion on these, based on preliminary analysis of the experiment data has also been presented. The data analysis was performed using MATLAB® environment (MATLAB, 2009).

Contents

List of Figures

List of Tables

Chapter 1

In vitro electrophysiology of neuronal networks: a historical perspective

1.1 Introduction

Humans are vastly superior to other animals in their ability to exploit their physical environment. The enourmous complexity and variability of the world surrounding us is received by the nervous system through a sophisticated array of sensory receptors: the brain's job consists in organizing the incoming sensory information in perceptions and elaborating an appropriate behavioral response. This task is accomplished by the brain using nerve cells (i.e. neurons) and the connections between them (i.e. synapses). Individual nerve cells, the basic units of the brain, are relatively simple in their morphology: although the human brain contains a thousand different types of neurons, they all share the same basic architecture (see Fig. 1.1). The complexity of human behavior depends less on the specialization of individual nerve cells and more on the fact that a great number of these cells form precise anatomical circuits. Hence, the capability of the nervous system to produce different actions in response to complex sensory stimuli derives from the way neurons are connected with each other and with sensory receptors and muscles, rather than single-cell specialization (Kandel et al., 2000).

In summary, four basic features of the nervous system responsible of the generation of behavior can be identified:

1. The mechanisms by which neurons produce signals.
2. The patterns of connections between nerve cells.
3. The relationship of different patterns of interconnection to different types of behavior.
4. The means by which neurons and their connections are modified by experience.

In this introductory chapter, we would like to outline some basics about how neurons produce propagating electrical signals (see §1.2) and how they establish interconnections between each other (see §1.3). In the following section, we report some brief notes about the methods neuroscientists use to investigate the function of neurons and synapses through different kinds of *in vitro* neural preparations (see §1.4). Finally, we dedicate an entire section to the description of state-of-the-art electrophysiological techniques, focusing on in–vitro applications and going from patch–clamp (see §1.5.1) to microelectrode arrays (MEAs) (see §1.5.2), which is the main tool exploited in the context of this thesis.

1.2 Neurons and glia

There are two main classes of cells in the nervous system: nerve cells (i.e. neurons) and glial cells (i.e. glia).

Glial cells

In the Central Nervous System (CNS) of vertebrates, the number of glial cells is 10 to 50 times the number of neurons (Kandel et al., 2000). One may ask the reason of such overabundance of glia: although glial cells are not excitable, as neurons are, they carry out several vital roles. They provide to neurons structural and metabolic support, protection from pathogens and other toxic substances, production of the axons' myelin sheath and removal of dead cells (Kandel et al., 2000). More recently, several studies about the role of astrocytes – the most numerous class of glial cells in the CNS – in modulating neuron function and synaptic plasticity have been published (Fellin, 2009).

Neurons

A typical neuron has four morphologically defined regions (see Fig. 1.1)

- **The cell body or soma**: it is the metabolic center of the cell, it contains the nucleus (where genes are stored) and the endoplasmic reticulum (where proteins are synthesized).
- **The dendrites**: dendrites branch out from the soma in a tree-like fashion and are the main apparatus for receiving incoming signals from other nerve cells.
- **The axon**: it extends away from the cell body and is the main conducting unit for carrying signals to other neurons.
- **The presynaptic terminals**: the chemical synapse is the point at which two neurons communicate and involves a presynaptic cell, which transmits a signal, and a postsynaptic cell, receiving the signal. The presynaptic terminal is a specialized cell compartment in which the electrical signals (i.e. action potentials) traveling through the axon are transduced in a chemical signal (i.e. neurotransmitter release)

captured by the postsynaptic receptors present in the dendrites. This chemical signal is again translated in an electrical one, affecting the postsynaptic neuron's membrane potential (see §1.3), and thus accomplishing the synaptic transmission.

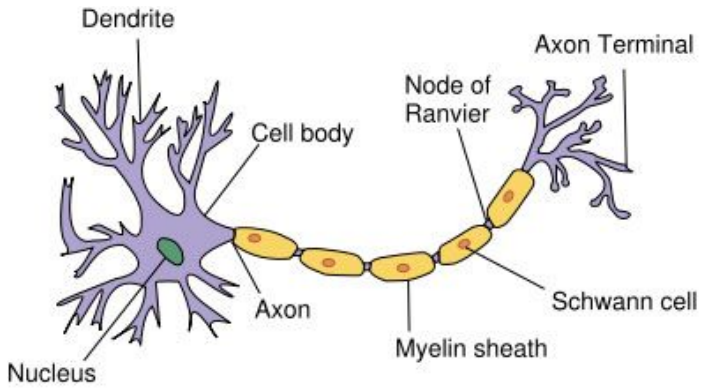

Figure 1.1: Simplified sketch of a neuron.

Mechanisms of action potential generation

At rest, all nerve cells maintain a difference in the electrical potential (V) on either side of the plasma membrane: this is called the resting membrane potential and in a typical neuron it is about -65 mV ($V = V_{intracellular} - V_{extracellular}$). The difference in electrical potential when the cell is at rest results from two factors:

1. The unequal distribution of electrically charged ions, in particular the positively charged Na^+ and K^+ ions and the negatively charged aminoacids and proteins on either side of the cell membrane.

2. The selective permeability of the membrane to just one of these ions, K^+. The unequal distribution of positively charged ions on either side of the plasma membrane is maintained by the Na^+ – K^+ pump, a membrane protein that pumps Na^+ out of the cell and K^+ back into it, keeping the Na^+ ion concentration in the cell low and the K^+ ion concentration high (see Table 1.1). At the same time, the cell membrane is selectively permeable to K^+, through specific membrane proteins (i.e. ion channels) highly permeable to K^+ and considerably less permeable to Na^+ (Kandel et al., 2000).

Excitable cells, such as neurons, differ from other cells in that their membrane potential can be significantly and quickly altered: this rapid change can serve as a signaling mechanism and is called the action potential. The action potential is composed of a rising phase (depolarization), followed by a falling phase bringing the membrane potential V down to a hyperpolarization phase. This shape is due to the activity of voltage-controlled channels of the membrane that modify the Na^+ and K^+ ion permeability as a function of the membrane potential (see Fig. 1.2).

Ion	Extracellular[mM]	Intracellular[mM]
Na^+	440	50
K^+	20	400
Cl-	560	52
A- (organic ions)	-	385

Table 1.1: Concentrations in mM of the major ions at the resting equilibrium inside and outside the cell (Kandel et. al, 2000).

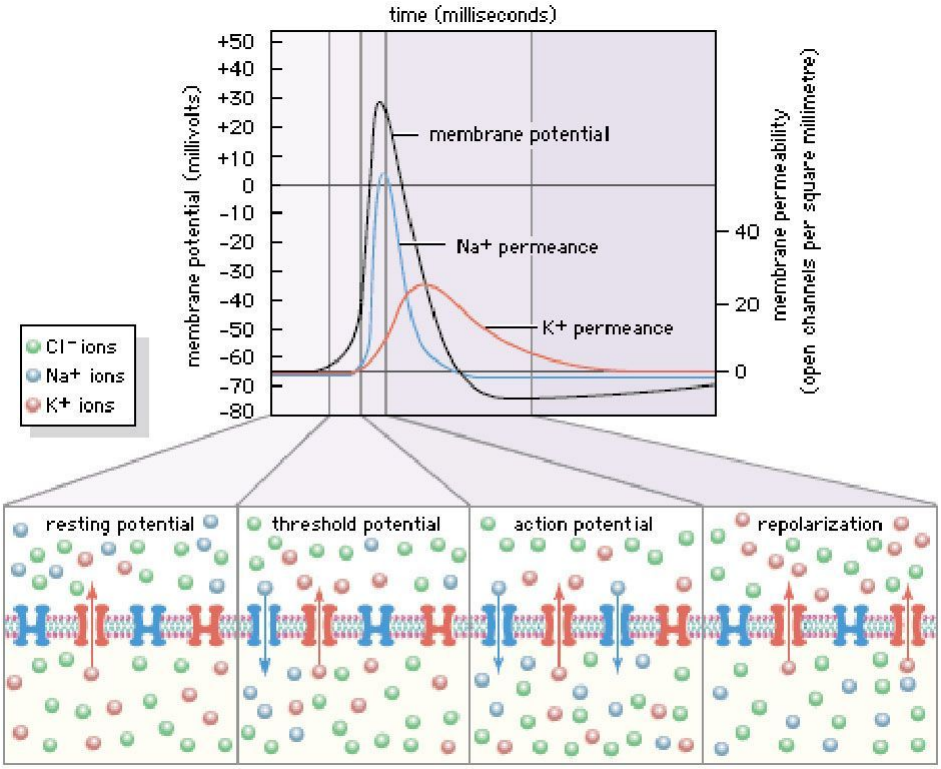

Figure 1.2: Scheme of action potential generation: Flow of Na^+ and K^+ ions through voltage-gated channels across the plasma membrane.

Briefly, when the neuron receives an input (synaptic or sensory, mediated by receptors) an influx of Na^+ or $Ca_2{}^+$ ions depolarizes the membrane: when the depolarization exceeds a critical threshold, the voltage-gated Na^+ permeable ion channels are open and V rapidly increases towards positive values. When V reaches its peak, the voltage-gated Na^+ channels close and, at the same time, the voltage-gated K^+ channels open, leading to a strong outflux of K^+ ions that re-establishes a negative membrane potential. The action potential is an all-or-none signal: this means that while stimuli below the threshold will not produce a signal, all stimuli above the threshold produce the same signal. Moreover, the amplitude and duration of each action potential are pretty much the same, regardless the stimulus' intensity or duration. Only two features of the conducting signal convey information: the number of action potentials and the time intervals between

them.

In summary, an action potential is an all-or-none signal, whose shape is stereotyped, and is produced by the movement of ions across the plasma membrane through voltage-gated channels.

1.3 The synapse

When an action potential reaches a neuron's terminal it stimulates the release of a chemical transmitter from the cell, as the neuron's output signal. In the CNS the major excitatory transmitter is L-glutamate, while the major inhibitory transmitter is γ-aminobutyric acid (GABA) (Kandel et al., 2000). Transmitter molecules are held in subcellular organelles called *synaptic vesicles*, which are loaded into specialized release sites in the presynaptic terminals called active zones. To unload their content, the vesicles fuse with the plasma membrane, a process known as exocytosis. After the transmitter is released from the presynaptic neuron, it diffuses across the tight space that separates the presynaptic and postsynaptic terminals (i.e. synaptic cleft) and it binds the corresponding receptors in the membrane of the postsynaptic neuron (see Fig. 1.3). The binding of transmitter to receptors causes the postsynaptic cell to generate a synaptic potential. Whether the synaptic potential has an excitatory (i.e. depolarizing) or inhibitory (i.e. hyperpolarizing) effect will depend on the type of receptors in the postsynaptic cell, not on the particular neurotransmitter (Kandel et al., 2000).

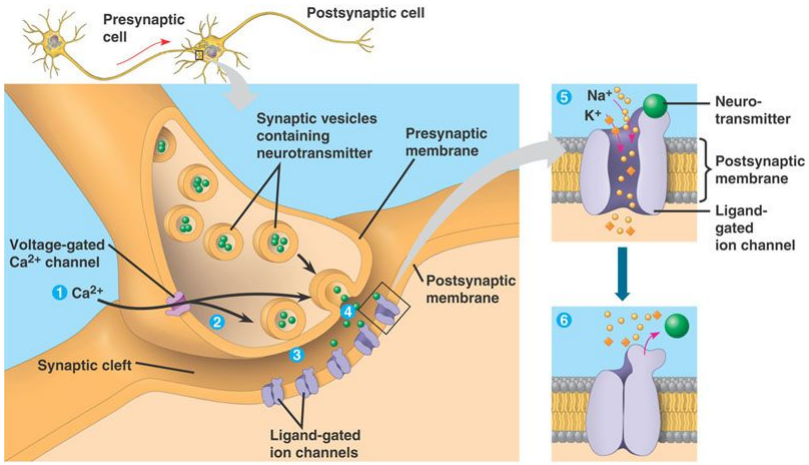

Figure 1.3: Model of a synapse.

1.4 *In vitro* neural preparations

In the early 1900's, the first studies in neurobiology employing tissue cultures were performed by Ross Granville Harrison (Harrison, 1907; Harrison, 1912): he examined the outgrowth of fibers from fragments of frog and chick neural tube cultured in drops of

clotted lymph or plasma and demonstrated for the first time that nerve fibers arise as outgrowths from individual nerve cell bodies (Banker and Goslin, 1998). These studies opened the way to the use of tissue cultures' techniques to address biological problems and attracted many followers (Carrell and Burroughs, 1910). In the following decades, together with the development of new approaches to cell culture methods (i.e. development of clonal cell lines of neuroblastoma cells and novel techniques to culture dissociated neurons, (Augusti-Tocco and Sato, 1969; Bray, 1970)) and the advancement of technology (e.g. microscopy techniques, (Zernike, 1934)), in vitro culturing began to gain a more prominent and important position in neurobiology.

Today, tissue culture is an integral part of modern neurobiology: nearly one third of the papers that currently appear in *Neuron* use nerve cell cultures as an important method (Banker and Goslin, 1998).

Cultures of dissociated neurons

When cells from the embryonic brain of animals are dissociated and placed into culture, neurons that have completed division *in situ* will extend processes, form synapses with one another and become electrically active. Differently from most types of tissues, even if tissue is removed at a time of active neurogenesis, it is rare to observe cells that divide in culture and subsequently acquire a neuronal phenotype. Such kind of cultures is referred to as primary cultures, because they are prepared from cells taken directly from the animal: the cells divide or not depending on the original tissue, acquire differentiated characteristics and ultimately die, but for the next experiment another animal has to be sacrificed in order to obtain new tissue and prepare new cultures.

Alternatively, it is possible to use continuous cell lines, mostly derived from tumor cells (e.g. mouse neuroblastoma tumor C-1300) (Augusti-Tocco and Sato, 1969): these cells can be sub-cultured repeatedly and express a reasonably stable phenotype. Comparing cell lines vs primary cultures is not the aim of this short introduction, not to mention the different fields of application. Briefly, one of the drawbacks of using cell lines is that they often do not express some key aspects of neuronal differentiation (e.g. development of axons and dendrites, formation of synapses, etc.), although they share a great many of the individual characteristics of differentiated neurons (e.g. neurotrasmitters, ion channels, receptors and other neuron-specific proteins) (Banker and Goslin, 1998).

In this thesis, for electrophysiology purpose, we made use of primary cultures of dissociated neurons from rat embryos, plated at a relatively high density (1200 cells/ μl) onto planar MEAs. In what follows, we briefly describe the procedure used to obtain and maintain the cultures.

Neuronal cultures are obtained from cerebral cortices of embryonic rats, at gestational day 18 (E18). The cerebral cortices of 4–5 rat embryos are dissected and then exposed to chemical (0.125% trypsin solution for 20 minutes at 37 °C) as well as mechanical dissociation (through flame-narrowed Pasteur pipettes). The resulting tissue is resuspended in Neurobasal medium (Invitrogen, Carlsbad, CA, USA), supplemented with 2% B27 (Brewer, 1997; Brewer et al., 1993) and 1% Glutamax-I (both Invitro-

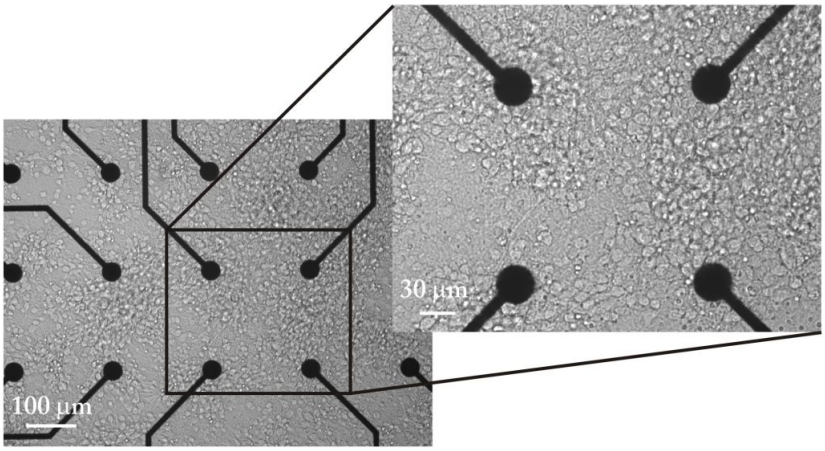

Figure 1.4: Image of a cortical network cultured over an MEA for 24 days *in vitro* at two magnifications (10x and 20x, calibration bars: $100\mu m$ and $30\mu m$).

gen) at the final concentration of about 1,200 cells/μl. Cells are then plated onto the substrates, precoated with adhesion promoting molecules (first laminin, 50 $\mu g/ml$, and second poly-D-lysine, 100 $\mu g/ml$, both from Sigma–Aldrich), at the estimated density of 48,000-50,000 cells/device. The cultures are maintained in MEA devices, each containing 1 ml of nutrient medium (i.e. serum-free Neurobasal medium supplemented with 2% B27 and 1% Glutamax), in a humidified incubator having a controlled atmosphere (5% CO_2, balance air) at 37°C. No antimitotic drug, that prevents glia proliferation, was added in our cultures, (Araque et al., 1999; Nedergaard, 1994; Pfrieger and Barres, 1997) because of the essential role played by glial cells in the nervous system (see §1.2). Half of the medium is replaced once a week until the 4th week in vitro and twice a week afterwards. The cultures can be kept in healthy conditions for several weeks and after 3-4 weeks *in vitro* they reach a mature developmental stage, characterized by quasi -synchronous array-wide bursts, mixed with isolated random spikes (Chiappalone et al., 2006; van Pelt et al., 2004). In Fig. 1.4, a network of rat cortical neurons at 24 DIV over an MEA is shown at different magnifications.

Brain slice preparation

Instead of dissociate cells from the neural tissue, an alternative approach can be adopted that allows to partially keep the 3D structure of the intact brain in vitro: slices of brain can be cut from different areas - hippocampus alone or together with entorhinal cortex, cerebellum, cortex, striatum, etc. - and can be kept alive for several hours in various media (acute slices) or maintained in culture for days/weeks (organotypic slice cultures).

Brain slices allow recording from semi-intact neural circuits, with the advantages of mechanical stability and control over the extracellular environment. These preparations are often used for a wide variety of studies, including synaptic plasticity and development, network oscillations, intrinsic and synaptic properties of defined neuronal populations, and many others (Kettenmann and Grantyn, 1992). Depending on the experimental needs several variants of the technique have been developed and are being

used. One distinction between the variants relates to how thick the slices have been cut. The thin slice technique was developed to allow visualization of individual cells in slices less than 250 μm, while the thick slice technique is used in experiments where connectivity and maintenance of normal dendritic structure are crucial for the study.

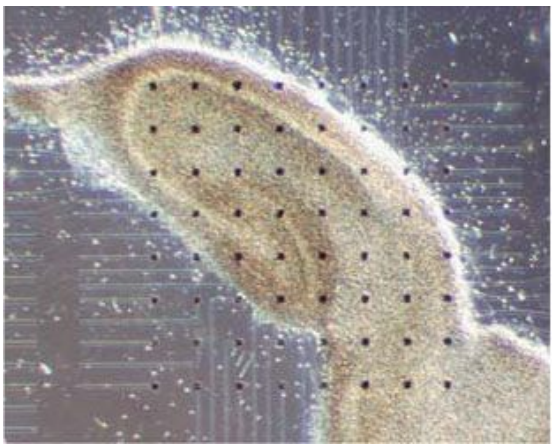

Figure 1.5: Hippocampal slice from an 11-day-old rat, cultured and maintained on MED64 probes (Alpha Med Scientific Inc., Japan). (From (Shimono et. al., 2000))

The culturing of organotypic brain slice cultures have been based on earlier work on explant cultures derived from different anatomical region reviewed by Crain (Crain, 1976), and became an increasing popular tool with the development of the roller-tube technique in 1981 by Gähwiler (Gähwiler, 1981) and later the interface cultures in 1991 by Stoppini (De Simoni and Yu, 2006; Noraberg et al., 1999; Stoppini et al., 1991) and Yu, 2006; Hippocampal/cortical slice cultures have also been coupled to planar MEAs (Beggs and Plenz, 2003) and Plenz, 2003; (Egert et al., 1998; Jahnsen et al., 1999), thus allowing long-term extracellular measurements of defined neuronal circuits.

1.5 State-of-the-art of recording and stimulation techniques

Different techniques exist for measuring and evoking the electrophysiological activity of in vitro neuronal networks: a first distinction can be made between intracellular and extracellular techniques.

- **Intracellular technique**: Previously, the action potential - the main feature of nerve cells' electrophysiological activity - has been described considering the ionic flows across the cellular membrane: the direct measurement of the potential difference across the membrane needs two measuring points, one in the cell and the second outside. This kind of electrophysiological measurement is called intracellular technique and requires the breaking of the membrane.

- **Extracellular technique**: Alternatively, one can place the first measuring point outside the cell, but very close to the membrane, and the second one, the reference,

far away from the cell. As described above (see §1.2), when an action potential occurs, the intracellular and extracellular ionic concentrations are both modified by the membrane transport properties: the extracellular changes are localised near the membrane and currents entering or leaving a neuron generate voltage signals at the electrode nearby. This results from a resistive drop in the medium between the reference electrode and the recording electrode. This measurement technique has been referred to as extracellular technique.

Intracellularly and extracellularly recorded signals are very different. Not only the amplitude of extracellular signals is lower than that of intracellular ones (20 – 200 μV_{pp} for a typical action potential of 100 mV_{pp} measured intracellularly), but also the shape is different. Models of the neuron- microelectrode junction have been developed (Martinoia et al., 2004a) in order to better understand and correctly interpret the extracellular traces recorded from neuronal populations. A coupling stage taking into account several parameters of the junction allows to reproduce the low-pass filtering effect introduced by the extracellular measurement. The main variables involved in the signal transduction are the *sealing resistance* R_{seal}, depending on the relative area of the microelectrode covered by the cell and the distance between the cell and the microelectrode, and the *cell membrane-electrolyte capacitance* C_{hd}, modeling the polarization layers of the electrolyte solution in front of the cell and in front of the microelectrode.

A neuron can be excited intracellularly by injecting a current directly into it, but also an extracellular stimulation can be realized by applying a voltage or a current to the extracellular electrode. Application of voltage to the electrodes charges the capacity of the electrical double layer of the metal-electrolyte interface. This leads to fast, strong, but transient, capacitive currents with opposite sign at the rising and falling edges of voltage pulses resulting in transient hyperpolarization and depolarization of cellular membranes (Fromherz and Stett, 1995; Stett et al., 2000). This is similar to the effect of brief biphasic current pulses commonly used for safe tissue stimulation (Tehovnik, 1996). In both cases, however, membrane polarization of the target neurons is primarily affected by the voltage gradient generated by the local current density and tissue resistance in the vicinity of the cells (Fejtl et al., 2006).

1.5.1 The patch-clamp technique for single-cell electrophysiology

In vitro electrophysiology has seen the majority of its development using glass pipette electrodes. Neurophysiologists have studied single-cell properties, ion channels, drugs' effects and synaptic signalling with these electrodes (Kettenmann and Grantyn, 1992). The electrodes are made by pulling a glass tube into a fine capillary at one end (less than μm in diameter) and filling it with a saline solution, whose composition matches with either the composition of the cytoplasm or of the bath solution, depending on the chosen configuration. Finally an electrode, typically platinum or Ag/AgCl, electrically contacts the solution to the measuring circuit. Glass pipettes are used in different configurations: intracellular, extracellular or patch-clamp. The patch-clamp technique was proposed

for the first time by Erwin Neher and Bert Sakmann in the late 1970s and they won the Nobel Prize in Physiology or Medicine in 1991 for this work. This technique is a refinement of voltage clamping and was developed in order to record current flow from single ion channels. The electrodes used for patch are distinct from the sharp microelectrodes used to impale cells in traditional intracellular recordings, in that they are sealed onto the surface of the cell membrane, rather than inserted through it. In some experiments, the micropipette tip is heated in a microforge to produce a smooth surface that assists in forming a high resistance seal with the cell membrane. After leaning the pipette against the cell membrane, a small amount of suction is applied to the patch pipette in order to increase the tightness of the seal between the pipette and the membrane. The high seal lowers the electronic noise and allows to record very small currents across the patch of membrane under the pipette, including those produced by ion channels with very small conductances (Kandel et al., 2000).

Several variations of the basic technique can be applied, depending on what the researcher wants to study. The inside-out and outside-out techniques are called excised patch techniques, because the patch is excised (i.e. removed) from the main body of the cell. They are different in which side of the membrane's patch is exposed to the external medium. In the cell-attached configuration the electrode is sealed to the patch of membrane and the cell remains intact, allowing to record currents through single ion channels in that patch of membrane. Whole-cell recordings, in contrast, involve recording currents through multiple channels at once, over the membrane of the entire cell. The electrode is left in place on the cell, but more suction is applied to rupture the membrane patch, thus providing access to the intracellular space of the cell. Cell-attached and both excised patch techniques are used to study the behavior of individual ion channels in the section of membrane attached to the electrode. Differently, whole-cell patch allows the researcher to study the electrical behavior of the entire cell.

1.5.2 Microelectrode arrays for network electrophysiology

In 1972, Thomas at al. published the first paper describing a planar MEA for use in recording from cultured cells (Thomas et al., 1972). In their introduction, they underlined that "the most interesting questions to be asked of such cultures are those dealing with the development and plasticity of electrical interactions among the cultured elements tissues or single cells)" (Thomas et al., 1972). They also clearly stated that the "exploration of these questions would be greatly facilitated by a convenient non-destructive method for maintaining electrical contact with an individual culture, at a large number of points, over periods of days or weeks". More than 30 years ago, they charted a course for the years to come, identifying which directions of investigations to pursue and also delineating possible ways.

The MEA that was developed had two rows of 15 electrodes each, spaced 100 μm apart, and was intended for experiments with cultured chick dorsal root ganglion neurons. The array was on glass, with gold electrodes and leads over an adhesion layer, insulated with photoresist. The electrodes were plated with platinum black to reduce the impedance of their connection to the culture medium (Robinson, 1968) and were 7

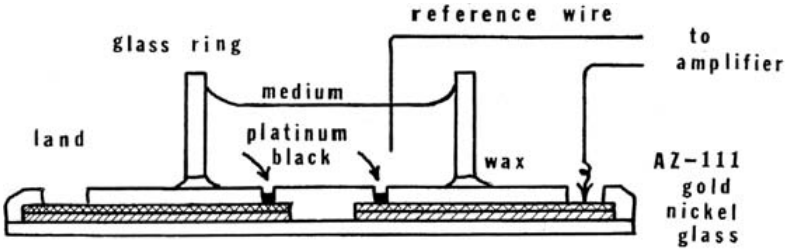

Figure 1.6: Schematic diagram of the MEA structure. (From Thomas et. al, 1972)

μm square (see Fig. 1.6). Although initial experiments were unsuccessful, turning to dissociated chick myocytes they found it possible to record robust electrical signals (200 – 1000 μV in amplitude).

Five years later, in 1977, with a very similar introduction to that of Thomas at al., Guenter Gross and his collaborators proposed the idea of an MEA, without knowledge of the previous work (Gross et al., 1977). They showed recordings from an isolated snail ganglion laid over the electrodes, with single action potentials having amplitudes up to 3 mV , depending upon the cell size.

The first successful recordings from single dissociated neurons using an MEA were reported by Pine in 1980 (see Fig.1.7): he succeeded in recording from a network of rat superior cervical ganglion neurons, cultured for up to three weeks over an MEA with 32 gold electrodes (two parallel lines of 16 electrodes each, 10 square and 250 μm apart), platinized and insulated with silicon dioxide (Pine, 1980). He also used the same MEA for stimulating neurons with a voltage pulse of 0.5 V and duration of 1 ms. These three works put a milestone for the upcoming work and marked the beginning of in vitro network electrophysiology using MEAs.

In the 1980's, many studies employing MEAs for different purposes followed. While some were looking for alternative (and promising) new technical solutions (i.e. Field effect transistor-based MEAs, first proposed in 1981 by Jobling et al. (Jobling et al., 1981)), some others exploited these new tools to investigate either the network activity of cultures of dissociated neurons (Gross et al., 1982) or of hippocampal slice preparations (Wheeler and Novak, 1986). Soon, it was clear that large invertebrate neurons were the most suitable to be plated on top of MEAs (Regehr et al., 1989): they are easily identifiable by their size and location in ganglia, can be dissected out, and can be used with other identified neurons to form simple networks in culture that replicate some or all of their connections in vivo. MEAs can provide a means for long-term noninvasive communication with such networks for stimulation and recording, much superior to conventional electrodes (Pine, 2006). Differently, at the end of the 1980s, Meister at al. coupled an explanted salamander retina to an MEA (and later on retinas from newborn ferrets and cats) and they could record spontaneous and evoked by light stimulation bursts of activity (Meister et al., 1989; Meister et al., 1994).

At the beginning of the 1990's, the combination of an MEA (for stimulation) and voltage sensitive dyes (for recording) was exploited to allow the detection and measurement of subthreshold synaptic potentials, otherwise impossible by recording extracellular

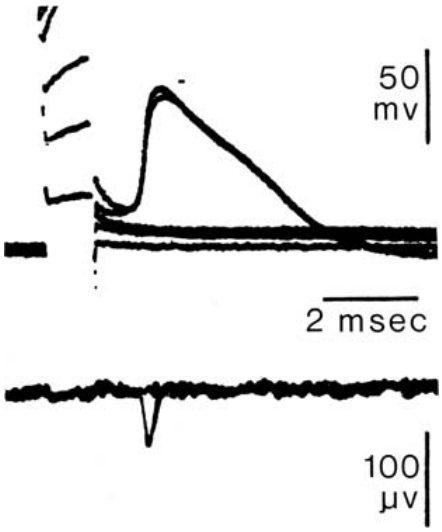

Figure 1.7: Five superimposed intracellular oscilloscope traces are at the top. Action potential signals are seen for the largest two. Below are extracellular recordings made simultaneously with the intracellular ones. The two below baseline are from the action potentials, and are too similar to resolve. (From (Pine, 1980))

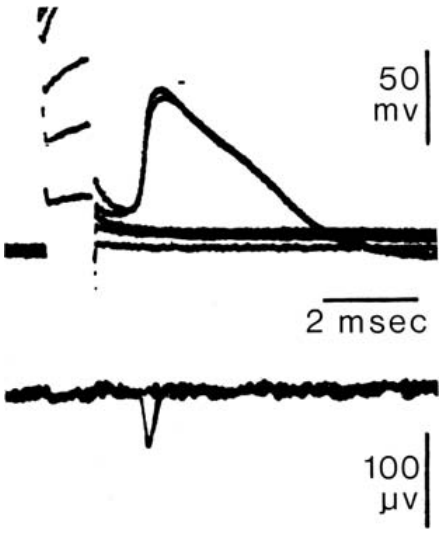

Figure 1.8: Dishwide bursting in a dense cortical culture. (From (Jimbo et al., 2000))

electrical signals (Chien and Pine, 1991). At the same time, Fromherz and his collaborators investigated the use of a field effect transistor (FET) to record action potentials from large Retzius cells of the leech (Fromherz et al., 1991), and this began a series of investigations in the Fromherz lab aimed at understanding the FET-neuron interface.

As originally foreseen by Thomas and collaborators (Thomas et al., 1972), network development and plasticity are the most interesting questions that can be addressed by using MEAs. These are the main goals pursued in the 1990's by groups in Japan at the Matsuhita and NTT laboratories, led by Taketani and Kawana: they fabricated

64-electrode MEAs for use in slice experiments (Oka et al., 1999) and with cultures of dissociated cortical neurons (Maeda et al., 1995) (see Fig. 1.8). For slices, a rocking device was developed for keeping cultured organotypic slices alive over many weeks, so that their development could be observed over time (Kamioka et al., 1997). For cortical cultures, experiments probed plasticity of connections as a result of tetanic stimulation (Jimbo et al., 1999). At the same time, Pine and collaborators were looking for new technical solutions to improve the coupling between neurons and microelectrodes, through a neuro-cage approach (Maher et al., 1999). Several of these studies, which provided promising preliminary results, have continued in the period from 2000 to the present. More recently, much of the attention of the scientific community has been focused on describing the ubiquitous spontaneous bursting activity present in almost all of in vitro preparations (Beggs and Plenz, 2003); (Eytan and Marom, 2006; Pasquale et al., 2008; Raichman and Ben-Jacob, 2008; Wagenaar et al., 2005; Wagenaar et al., 2006).

Moreover, innovative protocols for inducing network plasticity have been presented in the literature, partially inspired by the work of Jimbo and collaborators (Chiappalone et al., 2008; Shahaf and Marom, 2001). Since the 1990's (Gross et al., 1992; Gross et al., 1995), neuronal networks grown on planar MEAs have been considered as a promising tool for drug screening and neurotoxicity studies (Gramowski et al., 2000; Gramowski et al., 2004; Keefer et al., 2001): this approach has proven to be useful in quantifying changes in the network activity in response to different neuroactive compounds (Martinoia et al., 2005a; Martinoia et al., 2005b). Finally, the Potter group in Atlanta and, at the same time, the research group in Genova, led by Martinoia have developed systems for re-embodying cultured networks: they connected the culture in a closed-loop with an artificial body, either simulated on the computer (DeMarse et al., 2001) or represented by an actual robot (Bakkum et al., 2004; Martinoia et al., 2004b) (see Fig. 1.9). The main goal of this approach was to provide the neuronal network "natural" inputs from the outside, in order to overcome one of the essential limitations of the in vitro methodology, i.e. the lack of a bi-directional communication with the surrounding environment. Research is still going on in this direction, exploiting the robot-culture closed-loop architecture as a platform for studying plasticity and learning.

MEAs vs. traditional methods – advantages and limitations

During the last 30 years, the invention and the continuous improvement of planar multi-electrode array devices have made possible experiments unthinkable before the 1970's, exploring network-level phenomena (i.e. network physiology). At the same time, MEAs allow experiments that can also be performed with traditional non-MEA instrumentation, but are enhanced by the use of multi-electrode devices. However, although modern MEAs can in general perform all the major types of traditional experiments (involving either dissociated cell cultures or slices), they are not always the best choice for a particular application (Whitson et al., 2006). Determining MEA applicability requires careful consideration of their specific strengths and weaknesses. From a traditional perspective, their major strengths include:

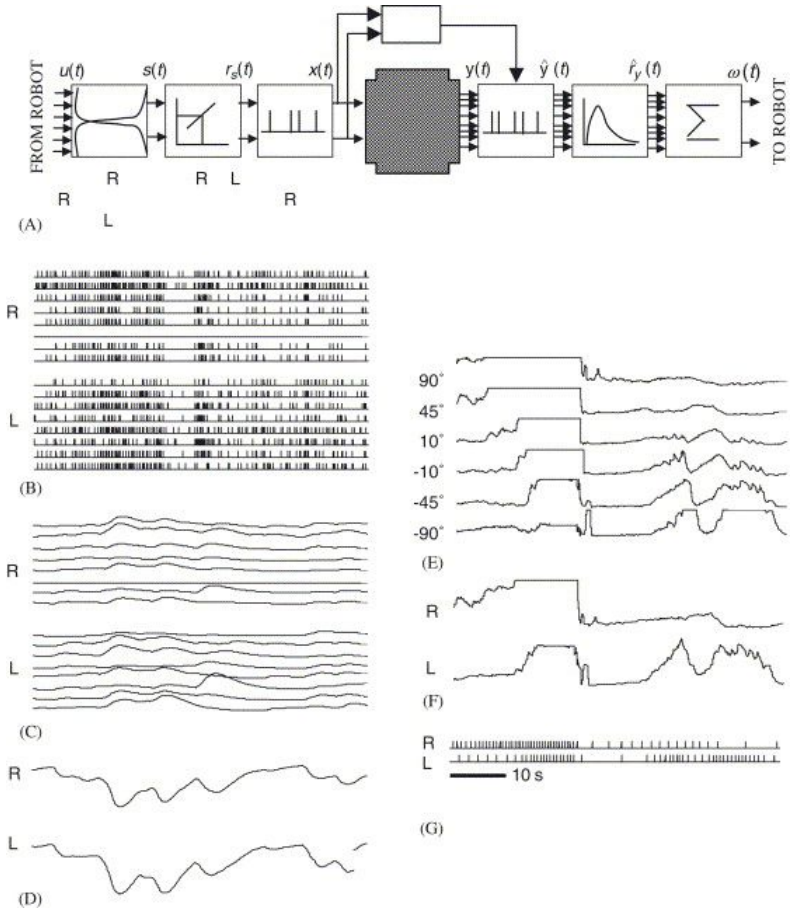

Figure 1.9: (A) Block diagram of the NeuroBIT project's bi-directional neural interface. (B-G) A 60-s portion of a typical closed-loop experiment: recorded spike trains (B) and instantaneous firing rates (C) from the 16 output sites, motor commands (D) and, on the right, the corresponding activity of the IR sensors (E), the average left and right sensor activity (F) and the corresponding pattern of stimulation (G). (From (Cozzi et al., 2005))

1. The ability to gather data from multiple sites in parallel as if running multiple experiments in a single culture/slice;
2. The ability to change stimulation and recording sites very quickly among those available in the array;
3. The ability to do away with the need to place multiple electrodes individually by hand;
4. The ability to increase culture sterility (either for dissociated cells or organotypic cultures).

Conversely, limitations include:

1. Smaller amplitude recordings (in most cases), as compared to traditional instrumentation because the electrodes are not inserted directly inside the cell;

2. Lesser independent mobility of the elctrodes, since they are arranged in a fixed pattern.

Only by exploiting the 2-D structure of MEAs it is possible to perform a spatio-temporal analysis of activity propagation patterns: for example, the use of MEAs allowed to capture the 2-D functional anatomy of the hippocampus (Shimono et al., 2000), by using a technique called 2-D current source density (2-D-CSD) analysis. This technique, made possible by 2-D MEAs, provides a clear picture of the concentration of currents into and out of neuronal regions, and allows to identify neuronal circuits in a brain's portion. Similarly, the availability of several recording points to monitor the network's activity is essential to evaluate the effects of plasticity protocols on the whole neuronal system (Chiappalone et al., 2008; Jimbo et al., 1999; Jimbo et al., 2000), defining long-term network potentiation (LTNP) or long-term network depression (LTND).

Considering the technological advances of the modern electronic industry (i.e. ever-increasing electronics miniaturization and machines' storage and computation capabilities), quite recently there has been a strong effort towards the production of high-density MEAs (Berdondini et al., 2009; Frey et al., 2009). In fact, one of the main limitations of currently commercially available MEAs is the low number of recording points when compared to the total number of cells in the network. Moreover, due to the high inter electrode distance (on the order of hundreds of μm for standard MEAs), it is necessary to plate cells at a relatively high density (about $2000 cells/mm^2$) to get a good covering of the electrodes. These issues has led to the search for an array with a very high number of embedded microelectrodes, whose size (and distance) is comparable to that of a neuron (Imfeld et al., 2008).

Chapter 2

Microelectrode arrays and the neuro–robotic architecture: technical description of the experimental set-up

2.1 Introduction

Nowadays, thanks to advances in electronic technology, commercial systems based on the microelectrode array (MEA) methodology are readily available. Actually, many neuroengineering laboratories all over the world are using this approach to study the laws which underlie the behavior of neuronal networks (Chiappalone et al., 2008; Eytan and Marom, 2006; Wagenaar et al., 2006). In the previous chapter, we outlined the history of MEA electrophysiology, starting from the very first applications to the most recent developments. Here, we would like to give further technical details about commercially available MEAs and the required experimental set-up.

2.2 Microelectrode array technology: standard devices

MEAs are made of cell-sized electrodes (10–100 μm diameter) placed onto a glass substrate. The electrodes, typically made of Au, Indium-Tin Oxide (ITO), Titanium Nitride (TiN), or black platinum, must be bio-compatible, long-term lasting, and preferably should have low impedance (less than 500 $k\Omega$ at 1 kHz) for low thermal noise.

The MEA non-sensitive surface and electrode leads are coated with bio-compatible insulators (e.g. polyamide or silicon nitride/oxide) which prevent short circuits with the electrolyte bath. These insulators, again coated with adhesion-promoting molecules, such as polylysine and/or laminin, allow and help the neuron coupling to the device surface. The low impedance of the electrodes, and the choice of a correct voltage range to avoid the generation of neurotoxic redox complexes, enable using them to deliver external

stimuli. The fabrication of MEAs is based on the thin-film technology (Elshabini-Riad and Barlow, 1998) and is realized in a clean-room, using standard photolithographic techniques.

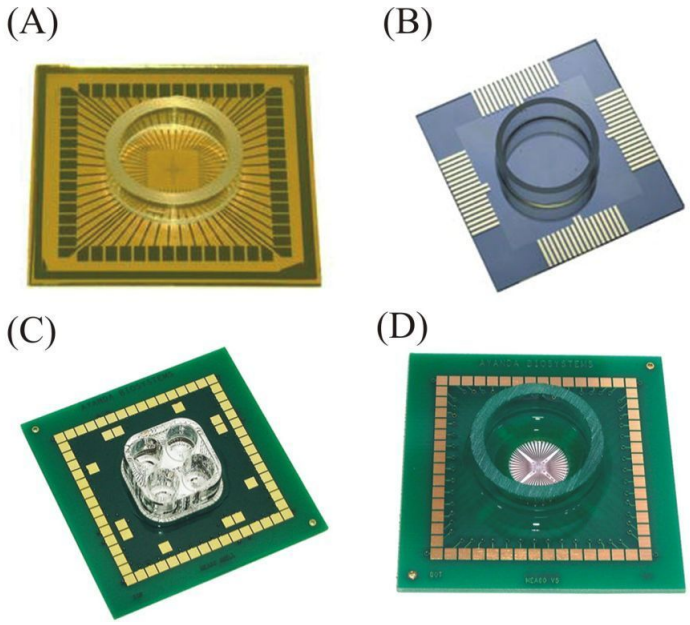

Figure 2.1: MEAs produced by different companies. (A) MEA 30/200 made by Multi Channel Systems for dissociated neuronal cultures, (B) MED60 made by Panasonic, (C) multi-well chip for pharmacological applications and (D) 3D electrodes for slice preparations, both made by Ayanda-Biosystems.

The rapid success met by MEAs in the neuroscience research field (see §1.5.2) moved some electronic companies to develop commercial systems to perform electrophysiological measurements using MEAs. At the present, there are on the market at least two complete acquisition systems based on MEAs: the MED System produced by Panasonic (`www.med64.com`, Osaka, Japan) and the MEA System produced by Multi Channel Systems (`www.multichannelsystems.com`, Reutlingen, Germany). Other companies, such as Ayanda-Biosystems (`www.ayanda-biosys.com`, Lausanne, Switzerland), and Plexon (`www.plexoninc.com`, Dallas, USA) have only developed the microelectrode devices, for several different applications (cultures, slices, cardiomyocytes, retinal cells, pharmacological screening, etc.). Fig.2.1 shows four samples produced by Multi Channel Systems, Panasonic and Ayanda.

All the experimental results involving standard commercial devices presented in this thesis were obtained from recordings performed on MEAs manufactured by Multi Channel Systems. The following sections deal with the description of this experimental set-up.

2.2.1 MCS microelectrode array design

Multi Channel Systems (MCS) provides different types (electrode size and inter-electrode spacing) of MEAs. The MEAs used in this work consist of 60 flat round electrodes made

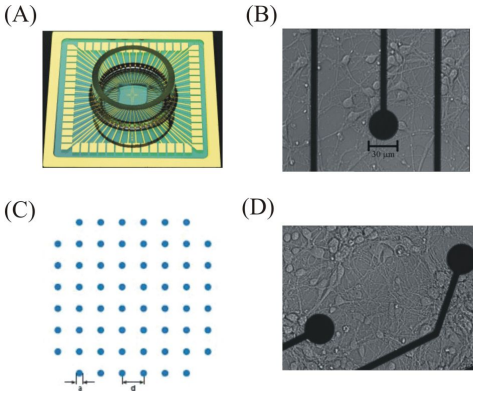

Figure 2.2: (A) Image of a typical MCS MEA, (B) 8x8 layout of an MCS MEA: a is the electrodes' size (e.g. 30 μm) and d is the inter-electrode spacing (e.g. 200 μm). (C) and (D) are optical images of a neuronal network over an MEA at 14 days in vitro (20x magnification).

of TiN. Tracks and contact pads are made of titanium or ITO, and the insulation material is silicon nitride (Si_3N_4). The electrodes are positioned in an 8x8 layout grid (the four corner electrodes are not present). ITO contact pads and tracks are transparent to allow a perfect view of the specimen under the microscope. Electrode diameters of either 10 μm or 30 μm are available, with an interelectrode distance of 30, 100, 200 or 500 μm (see Fig. 2.2). In this study we used only arrays of 30 μm electrodes, spaced 200 μm.

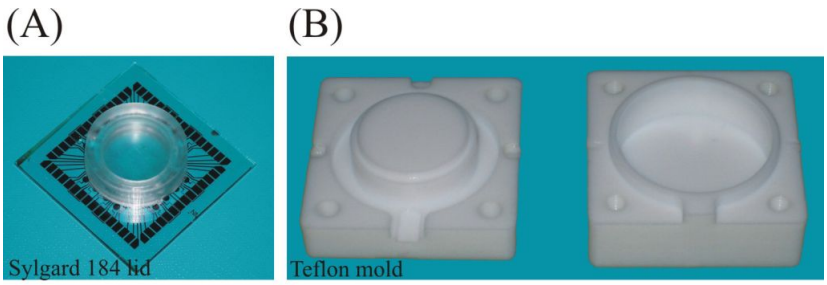

Figure 2.3: PDMS lid
(A) Image showing an MCS MEA covered by a PDMS lid, and (B) image of the two-part PTFE/FEP template used to mould the PDMS lids. PDMS has been purchased from Dow Corning (Sylgard 184 Silicone Elastomer Kit, `www.dowcorning.com`, Midland, MI, USA).

Latest generation MEAs are equipped with an internal reference electrode used to minimize the possibility of pollution that should be caused by the introduction of an external reference electrode. A glass ring is placed at the center of the devices, surrounding the recording area, and it allows to contain the culture medium (see §1.4). In this way, when placed in an incubator, the culture can survive for several weeks. There are various factors which may contribute to the gradual decline in the health of the culture, e.g. contamination by airborne pathogens or increase in the osmotic strength of the medium

due to evaporation. For these reasons, we made use of flexible polydimethylsyloxane (PDMS) lids in order to reduce the effects of these external factors (see Fig. 2.3) (Blau et al., 2009). PDMS is a biocompatible and transparent polymer that can be moulded and cured in a template (made of polytetrafluorethylene (PTFE/FEP) or poly(methyl methacrylate) (PMMA)) to get a proper shape: the peculiarity of PDMS is that it is permeable to gases (e.g. CO2, whose concentration at 5% is needed to maintain the medium's pH), but it greatly reduces evaporation, limiting the variation of the medium's osmolarity (Blau et al., 2009). Moreover, the PDMS lids prevent possible contamination by pathogens, thus allowing to record the same culture out of the incubator more than once. Finally, they can also include biocompatible tubing for continuous medium perfusion or an external Ag/AgCl reference electrode, preserving culture sterility.

2.2.2 The MCS MEA60 System

The Multi Channel Systems MEA60 set-up is made up of the following components, usually contained within a Faraday cage in order to reduce electro-magnetic interferences (see also Fig. 2.4):

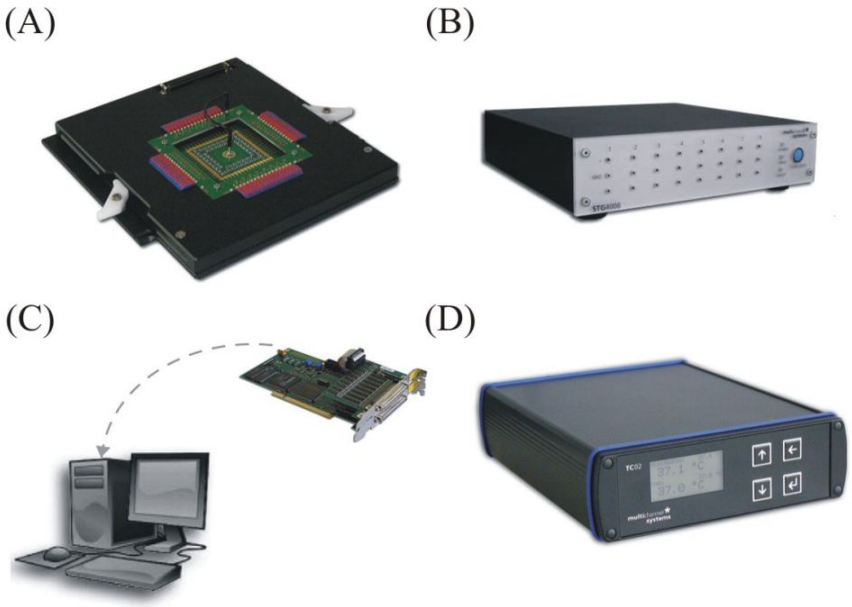

Figure 2.4: Multi Channel Systems set-up
Multi Channel Systems set-up: (A) MEA1060 amplifier, (B) MCS Stimulus Generator, (C) PCI-based acquisition card, (D) temperature controller.

- **Amplifier**: An amplifier stage for multi-electrode recording has to meet two main requirements:

  1. eliminating the cables connecting the electrodes and

2. coping with the interference (cross-talk phenomenon) among channels.

The MEA1060 60-channel amplifier has a compact design ($165 \times 165 \times 19\ mm$) and, due to the surface-mounted technology (SMD) of pre- and filter-amplifiers, the complete circuit and amplifier hardware was built into a single housing: this ensures optimal signal-to- noise ratio of the recording, because no further cables are necessary other than a single SCSI-type cable connecting the amplifier to the data acquisition card. This results in an overall low noise level of the complete amplifier chain ($\times$ 1200, 12-bit resolution, 10 Hz to 3 kHz) of $\pm 3\ \mu$V , which is well within the ± 5 to 10 μV noise level of the MEA TiN electrode. Hence, the MEA sensor is placed directly inside the amplifier and settled so as to fit the standard microscopes.

- **Temperature controller**: The MCS temperature controller (TC02) uses a Proportional Integrative Derivative (PID) based technology. The MEA temperature can vary in the range from room temperature to $^{+}50^{o}$C. The set-point temperature is reached within a range of 30 s to 5 minutes, depending on the recording system configuration.

- **PCI-based acquisition board**: Standard PC technology is used as the backbone of high-speed multi-channel data acquisition. The data acquisition card is based on PCI-bus technology and allows the simultaneous sampling of up to 128 channels at a sampling rate of 50 kHz per channel. It is possible to set the input voltage range from ± 400 mV to ± 4 V in the data acquisition software and this allows to use the full 12-bit resolution bandwidth for signals of any amplitude. Three analog channels and a digital I/O port are accessible, allowing the simultaneous acquisition of analog data, such as current traces from a patch clamp amplifier or temperature together with the MEA electrode data. The digital I/O port features trigger IN/trigger OUT functionality.

- **Acquisition software**: The MC Rack software allows to record simultaneously the electrophysiological activity from the 60 electrodes of the MEA, and monitor the raw data in a real-time mode. Different parameters can be extracted from the data streams and the results can be plotted, saved, and exported to other programs for further analysis.

- **Stimulus generator**: The MCS stimulus generator (STG2004) is a general-purpose stimulator which generates pulses to be delivered to stimulating electrodes (up to 4 for this model and up to 8 for upgraded models). Complex stimulus waveforms (both current and voltage) of arbitrary duration are designed by using the provided MCS stimulus software and then stored in the stimulus generator connected to the MEA. Stimuli are "tailored" by the user by specifying the desired pulse waveform defining parameters into a worksheet. The pulse waveform is then displayed and the stimulus protocol is downloaded to the stimulus generator via a serial communication port. The stimulus generator operates in both voltage and

current mode, and it is equipped with separate voltage and current outputs for each channel.

In an improved version of the MEA60 System, up to four amplifers, each hosting an MEA device, can be connected to the data acquisition card and 120 out of a potential 240 MEA electrodes can be monitored simultaneously. This allows the parallel recording of more than one sample, particularly useful if one wants to compare the effects of the same experimental protocol on different cultures at the same time. This scalable MEA60 System has been designed by MCS to answer the ever-growing demand in basic research and pharmaceutical applications for automation of experimental and data analysis procedures. In our lab at the Istituto Italiano di Tecnologia (IIT), we used an MEA120 System to record up to two cultures of dissociated neurons at the same time and double the number of monitored samples. More details on the complete MEA60 System are available in (Whitson et al., 2006) and references therein. Further technical specifications and data sheets can be found on `www.multichannelsystems.com`.

2.2.3 Custom fittings for the MCS MEA60 System

Perfusion control system

The standard MEA electrophysiology set-up can be also combined with a perfusion system. Generally, a continous flow of artificial CSF (ACSF), saturated with 95% O_2 and 5%CO_2, is necessary for maintaining acute slices functional during the MEA recording, while a continous perfusion of nutrient medium is not strictly necessary for culture maintenance during the experiment. Nevertheless, a perfusion control system, either automated or manual, can be also used to perfuse cultures at extremely low rates ($\approx$ 100 μl/h) for very long-term recordings (on the order of days/weeks) to stabilize the network's activity (Eytan and Marom, 2006) or to deliver/wash-out drugs during pharmacological tests.

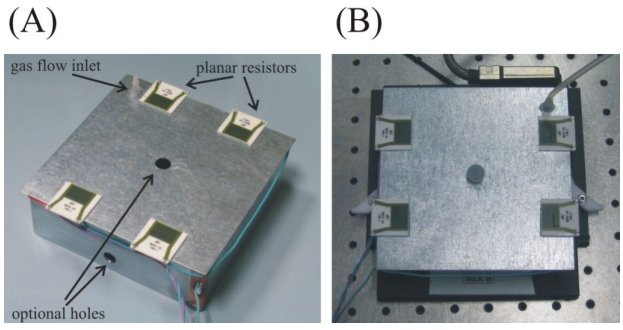

Figure 2.5: Custom recording chamber for MEA recordings
Custom recording chamber for MEA recordings. (A) Image of the recording chamber, highlighting the main features, and (B) image of the same chamber during normal operation over an MEA1060 amplifier.

Recording chamber

Within the incubator the temperature (37°C), the relative humidity (90-95%) and the CO2 concentration (5%) are controlled so as to maintain the culture medium pH ≈ 7.4 and the osmolarity ≈ 230 mOsm. In fact, large variations in these parameters strongly affect the network activity and, if permanent, can cause the culture death. Hence, the optimal recording conditions would be provided by the incubation environment, but actually it is not possible to store the MCS MEA1060 amplifier in a highly humidified atmosphere, as that of the incubator. This is the reason why we designed and realized a custom recording chamber, which, coupled to the use of a PDMS lid, allows the recording of cultures in safe conditions. The custom chamber (shown in Fig. 2.5) consists of a metallic box, sized 13× 13× 4 cm (W×L×H), heated on the topside through planar high-power ceramic resistors (BI Technologies, `www.bitechnologies.com`, Fullerton, CA, USA) and providing an inlet for a constant gas flow. In fact, the chamber is connected through PTFE/FEP tubing (Legris, `www.legris.com`, Rennes, France) to a gas cylinder containing a mix of 5% CO_2 - 20% O_2 - 75% N_2, practically the composition of air with 5% CO2: a constant slow flow of this gas mix into the metallic box covering the MEA during the experiment has been demonstrated to prevent the medium's pH to drift towards more basic values (up to 9 – 10 pH units) (Brewer et al., 2009a; Brewer et al., 2009b). Moreover, using this recording chamber, the MEA device containing the culture is not only heated bottom up by the amplifier's warming plate driven by the MCS temperature controller, but also top down through the ceramic resistors heating the metallic box. In fact, when supplied with a suitable voltage, they constantly heat the conducting metallic surface of the chamber so as to provide a surrounding environment for the MEA whose temperature (≈ 37°C) is homogeneous. This, together with the PDMS lid and with the fact that the gas is made bubble in water before being fed into the incubator, strongly reduces the evaporation and maintain the medium's osmolarity constant during the experiment. The recording chamber features a hole on the topside, to let the observation of the culture either using a microscope or to the naked eye, and a lateral hole, to let optional perfusion tubing in or out of the box. These holes are hermetically sealed during normal operation, to limit leakage and keep the 5% CO2 concentration and temperature as constant as possible inside the chamber. (Pasquale, 2009)

2.3 The Neuro–robotic architecture

In biological systems, high level cognitive functions, like learning, memory and processing of information emerge from the collective activity of large groups of neurons. These functions are present in different organisms, regardless of their complexity and anatomical structure. But wiring of the brain is also based on continuous interactions with the surrounding environment. The induction of mechanisms of neural plasticity, particularly in sensory-motor integration, is one of the primary processes bringing to network modification and consequently to reaction to the external world. For their complexity, biological structures cannot be fully translated into artificial systems. One of the most

relevant aspects in neuro-robotics is the possibility to study how to 'extract' the essential information embedded in a biological system, while maintaining a satisfactory level of neuronal complexity capable to support simple behaviors. In order to 'reproduce' a neural substrate (i.e. capable of mimicking basic brain functions) for artificial applications, hybrid model systems, where a set of living neurons are coupled with a robotic system, have been a possible choice in the recent past (DeMarse et al., 2001; Martinoia et al., 2004b; Mussa-Ivaldi et al., 2010). Such developed artificial systems were used to study sensori-motor feedback loops and plastic modifications of the neuronal substrate with respect to a supposed behavior (e.g., obstacle avoidance).

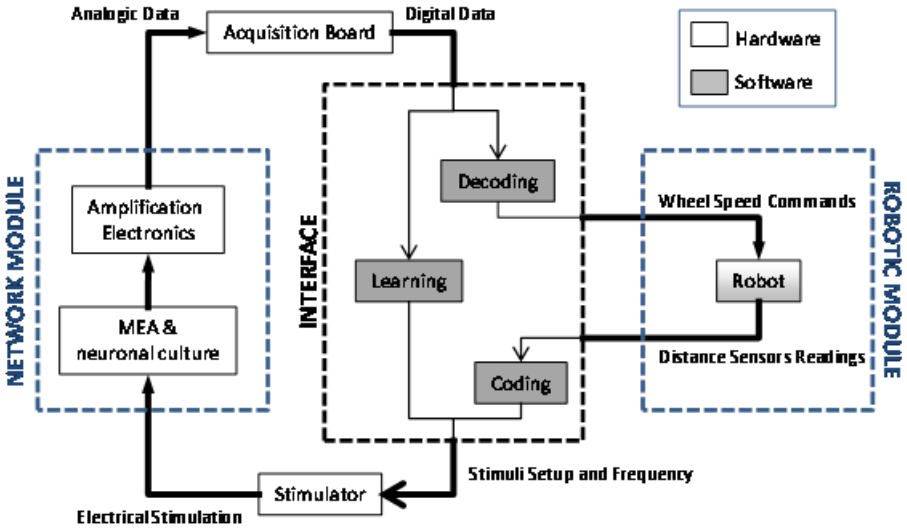

Figure 2.6: Block diagram of the neuro-robotic architecture
Block diagram of the neuro-robotic architecture. From left to right: (i) the network module, constituted by a network of living neurons coupled to a Micro Electrode Array; (ii) a computer which hosts the developed software tool (i.e. HyBrain) which manages the communication between the biological and the artificial part; (iii) the robotic module composed by a robot, either real or virtual, with sensors and actuators navigating into a circular arena with obstacles.

The neuro-robotic architecture includes several different elements (Fig. 2.6):

1. A network module, constituted by a neuronal culture over a MEA (i.e. the 'brain' of the neuro-robotic loop);

2. A computer, equipped with a data acquisition board, which hosts the developed software able to manage all the devices included in the architecture;

3. A stimulation unit, which is able to handle two different stimulation patterns. The stimulation signals are programmed via software and they are defined by their frequency, amplitude and stimulation site;

4. A robotic module, characterized by a small robot (either physical or virtual) with sensors and wheels able to move inside a circular arena with obstacles;

These different modules are synchronized and managed by a custom developed software named HyBrain which runs in the Windows environment (Mulas et al., 2010). Through this software, it is possible to control the parameters of the neuro-robotic experiments, namely the coding, decoding and learning schemes and all the required data processing. The network and robotic modules are described here. The interface block, designed entirely in software, will be discussed in Chapter 3.

2.3.1 Network module

Neuronal preparation

Dissociated neuronal cultures were prepared from cortices of 18-day old embryonic rats (pregnant female rats were obtained from Charles River Laboratories). Culture preparation was performed as previously described in 1.4.Recordings were performed on cultures between 25 and 35 DIVs.

Microelectrode arrays

Microelectrode arrays(Multichannel Systems, MCS, Reutlingen, Germany) consist of 59 TiN/SiN planar round electrodes (30 m diameter; 200 m center-to-center interelectrode distance) arranged in an 88 square grid excluding corners. One recording electrode is replaced by a larger ground electrode. Each electrode provides information on the activity of the neural network in its immediate area. A microwire connects each microelectrode of the MEA to a different channel of a dedicated amplifying system with a gain of 1100. The amplified, analogic, 60-channel data is then conveyed to the data acquisition card which samples them at 10 kHz per channel and converts them into digital, 12 bit data.

2.3.2 Robotic module

The robot, either virtual or physical, is basically a two-wheeled sensor platform: six infrared sensors are mounted on the robot at different angles, providing information about the distance of surrounding obstacles in different directions, whereas the speed profile of each wheel determine the direction and velocity of the robot itself. For the experiments in this thesis, the robot was tested using 'Random-turn experiments'. The specifics of these experiments are detailed in Chapter 4 (see §4.2.3). A typical experiment with the virtual robot is shown in Fig. 2.7: the robot is shown moving in a 200×200 pixels arena, where dark green pixels represent arena walls, which serve as obstacles to the robot. The light green pixels are free for the robot to move in. The robot (small pink circle in the left side of the arena) is collecting information about its environment through its six sensors: each black line departing from the robot represents the line of sight of a different sensor; their angles are fixed with respect to the robot heading (in this case, 30^o, 45^o and 90^o on both sides of the robot direction), while the length of each line is equal to the distance from the robot center to the closest wall in the sensor direction. This distance defines the reading of the sensor: the output is 0 if the robot is in direct contact with a wall, 1 if the closest wall is at the maximum distance possible.

The three sensor readings on each side are averaged to provide the neuronal network with a single value per side.

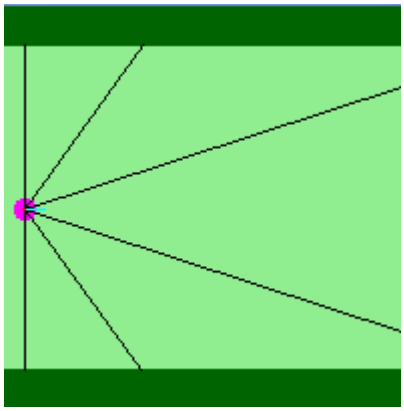

Figure 2.7: The robotic module
The robotic module: the simulated robot (pink circle) with its sensors (black lines departing from the robot) within the virtual arena. The red line represents the trajectory followed by the robot.

In the case shown in fig. 2.7, the robot is performing a random-turn experiment. The speed of a wheel is inversely proportional to the average of the sensor readings on the same side, thus the robot turns away from close obstacles. The task shown above is achieved trough a simple algorithm devised by Braitenberg (Braitenberg, 1984): in this application neither information is lost nor is there any significant delay between sensor data collection and motor command execution. Obtaining a behavior as close as possible to this one is the goal of the coding-decoding-learning process implemented here. During experiments, collisions with walls are unavoidable: following such an event, the robot moves back to a previous position in its path, at a fixed distance from the obstacle location.

Chapter 3

Online coding and decoding schemes

3.1 Introduction

This chapter describes in detail, the interface block in the neuro-robotic architecture (see fig. 2.6). As mentioned before, the interface block was designed completely in software. A custom software, named *HyBrain* was designed at IIT Genova in C#. A quick review of the signal features (namely, spikes and bursts) used to design the coding and decoding schemes have been included here. The coding and decoding schemes, both the old and the one proposed as part of thesis has been discussed. In addition, a simplified offline version of *HyBrain*, designed during the course of this thesis has been briefly introduced.

3.2 Spikes

The action potential in a neuron, also called "nerve impulse" or "spike", is a dramatic redistribution of electrical charge across the membrane. Action potentials result from the presence in a cell's membrane of special types of voltage-gated ion channels. A voltage-gated ion channel is a cluster of proteins embedded in the membrane that has three key properties:

1. It is capable of assuming more than one conformation.
2. At least one of the conformations creates a channel through the membrane that is permeable to specific types of ions.
3. The transition between conformations is influenced by the membrane potential.

Thus, a voltage-gated ion channel tends to be open for some values of the membrane potential, and closed for others. In most cases, however, the relationship between membrane potential and channel state is probabilistic and involves a time delay. Ions channels switch between conformations at unpredictable times: The membrane potential determines the rate of transitions and the probability per unit time of each type of transition.

The most intensively studied type of voltage-dependent ion channels comprises the sodium channels involved in fast nerve conduction. These are sometimes known as Hodgkin-Huxley sodium channels because they were first characterized by Alan Hodgkin and Andrew Huxley in their Nobel Prize-winning studies of the biophysics of the action potential. For a detailed explanation of the biophysics of action potential, see §1.2 and Fig. 3.1.

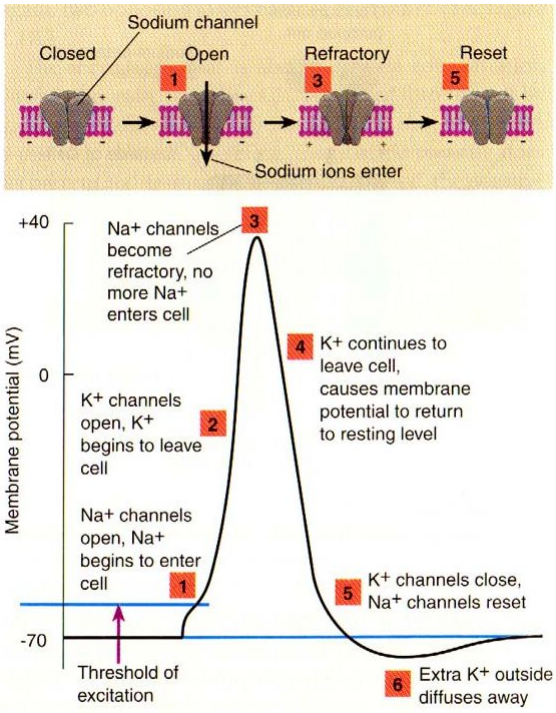

Figure 3.1: Various phases as the action potential passes a point on a cell membrane.

Currents produced by the opening of voltage-gated channels in the course of an action potential are typically significantly larger than the initial stimulating current. Thus, the amplitude, duration, and shape of the action potential are determined largely by the properties of the excitable membrane and not the amplitude or duration of the stimulus. This all-or-nothing property of the action potential sets it apart from graded potentials such as receptor potentials, electrotonic potentials, and synaptic potentials, which scale with the magnitude of the stimulus. A variety of action potential types exist in many cell types and cell compartments as determined by the types of voltage-gated channels, leak channels, channel distributions, ionic concentrations, membrane capacitance, temperature, and other factors.

3.2.1 Spike detection

The electrophysiological signals acquired from MEA electrodes must be preprocessed in order to remove the stimulus artifact and to isolate spikes from noise. The spike

detection algorithm uses a differential peak-to-peak threshold to follow the variability of the signal and a set of controls are made in order to make the algorithm as reliable as possible(Maccione et al., 2009). The threshold is proportional to the noise standard deviation (SD) and is calculated separately for each individual channel (typically as 6 or 7 times SD) before the beginning of the actual experiment.

3.3 Bursts

Bursting is an extremely diverse[1] general phenomenon of the activation patterns of neurons in the central nervous system and spinal cord where periods of rapid spiking are followed by quiescent, silent, periods. Bursting is thought to be important in the operation of robust central pattern generators, the transmission of neural codes, and some neuropathologies such as epilepsy. The study of bursting both directly and in how it takes part in other neural phenomena has been very popular since the beginnings of cellular neuroscience and is closely tied to the fields of neural synchronization, neural coding, plasticity, and attention.

A burst can be thought of as a dynamic state where a neuron repeatedly fires discrete groups or bursts of spikes. Each such burst is followed by a period of quiescence before the next burst occurs. Bursting neurons are important for motor pattern generation and synchronization. Almost every neuron can burst if stimulated or manipulated pharmacologically. Many burst autonomously due to the interplay of fast ionic currents responsible for spiking activity and slower currents that modulate the activity.

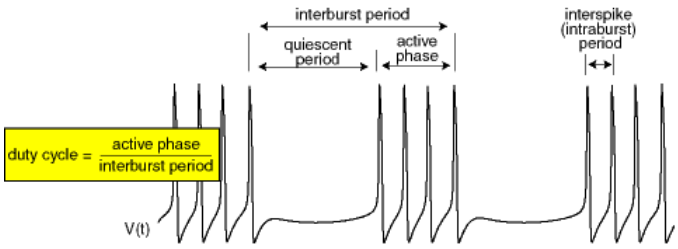

Figure 3.2: A bursting neuron (`www.scholarpedia.org/article/Bursting`).

3.3.1 Bursts as a unit of neuronal information

There are many hypotheses on the importance of bursting activity in neural computation.

- Bursts are more reliable than single spikes in evoking responses in postsynaptic cells. Indeed, excitatory post-synaptic potentials (EPSP) from each spike in a burst add up and may result in a superthreshold EPSP.
- Bursts overcome synaptic transmission failure. Indeed, postsynaptic responses to a single presynaptic spike may fail (release does not occur), however in response

to a bombardment of spikes, i.e., a burst, synaptic release is more likely (Lisman, 1997).

- Bursts facilitate transmitter release whereas single spikes do not (Lisman, 1997). Indeed, a synapse with strong short-term facilitation would be insensitive to single spikes or even short bursts, but not to longer bursts. Each spike in the longer burst facilitates the synapse so the effect of the last few spikes may be quite strong. Bursts evoke long-term potentiation and hence affect synaptic plasticity much greater than, or in a fashion much different from single spikes (Lisman, 1997).

- Bursts have higher signal-to-noise ratio than single spikes (Sherman, 2001). Indeed, burst threshold is higher than spike threshold, i.e., generation of bursts requires stronger inputs.

- Bursts can be used for selective communication if the postsynaptic cells have subthreshold oscillations of membrane potential. Such cells are sensitive to the frequency content of the input. Some bursts resonate with oscillations and elicit a response, others do not, depending on the interburst frequency (Izhikevich et al., 2003). Bursts can resonate with short-term synaptic plasticity making a synapse a band-pass filter (Izhikevich et al., 2003).

- Bursts encode different features of sensory input than single spikes (Gabbiani et al., 1996; Oswald et al., 2004). For example, neurons in the electrosensory lateral-line lobe (ELL) of weakly electric fish fire network induced-bursts in response to communication signals and single spikes in response to prey signals (Doiron et al., 2003). In the thalamus of the visual system bursts from pyramidal neurons encode stimuli that inhibit the neuron for a period of time and then rapidly excite the neuron (Lesica and Stanley, 2004). Natural scenes are often composed of such events.

- Bursts have more informational content than single spikes when analyzed as unitary events (Reinagel et al., 1999). This information may be encoded into the burst duration or in the fine temporal structure of inter-spike intervals within a burst.

In summary, burst input is more likely to have a stronger impact on the postsynaptic cell than single spike input, so some believe that bursts are all-or-none events, whereas single spikes may be noise! We were motivated by studies that argue that at a different level of analysis, information is spread out in the collective dynamics, the so-called "bursting" behavior (Gross, 1994; Tam, 2002; Tam and Gross, 1994). Accordingly, a simple algorithm for burst detection in real-time, for single channel spike trains has been developed.

3.3.2 Burst-detection

The detection of bursts in single channel spike trains hinges on a mathematically precise definition of the term "Burst". A theoretical definition of a spike burst was used as

proposed in (Chiappalone et al., 2005). Let $ST(t)$ be the spike train recorded from a single electrode (Perkel, 1967; Tam, 2002; Tam and Gross, 1994).

$$ST(t) = \sum_{n=1}^{N} \delta(t - t_n), \tag{3.1}$$

where N is the total number of spikes, t_n is the occurrence time of the n^{th} spike and $\delta(t)$ is a delta function denoting the occurrence of a spike at time $t = t_n$. The ISI is defined as the time interval between two consecutive spikes in the spike train.

$$ISI_n = t_n - t_{n-1} \tag{3.2}$$

We can now define bursts as sequences of densely packed spikes with a duration equal to the sum of the ISI within the burst and separated by an interval, called Inter-Burst Interval (IBI), that is relatively long compared to the burst duration (Tam, 2002). In this way, the burst train $BT(t)$ with a total number of M bursts, can be described as

$$BT(t) = \sum_{m=1}^{M} \left(A_m \Pi \left(\frac{t - t_m}{\tau_m} \right) \right) \tag{3.3}$$

where t_m denotes the starting time of the m^{th} burst in the $BT(t)$, $\Pi(t/\tau)$ is the rectangular function denoting the occurrence of a burst at time $t = t_m$ and lasting for time τ and A_m is the burst amplitude. The generic burst amplitude A_i can be calculated as

$$A_i = \frac{1}{\tau_i} \int_{\tau_i} \sum_{n=1}^{N_{\tau_i}} \delta(t - t_n) \mathrm{dt} = \frac{N_{\tau_i}}{\tau_i} \tag{3.4}$$

where τ_i is the burst time duration, N_{τ_i} is the number of spikes within that burst. It follows that the amplitude of a burst is given by the spike rate inside the burst, or equivalently, by two specific parameters such as the number of spikes per burst and the burst duration.

For burst detection, the spike train is analyzed in real time. Two thresholds were fixed: the first one is based on the statistical distribution of the spike train and is defined as the maximum ISI for spikes within a burst; the second one is defined as the minimum number of consecutive spikes belonging to a burst. The values of 100 ms and 5 spikes for maxISI and minSpikes respectively, were set after a series of comparisons between the results of the automated burst detection and the visual inspection of three experimenters (data not shown). Even if 100 ms can appear a high value, it has been shown to give better performance results, since each burst, especially in the early developmental stages, presents a long tail with lower frequency components, which must be included as part of the burst itself.

In summary, spike bursts are defined as sequences of spikes with each ISI smaller than the maxISI, and containing at least a number of spikes equal to minSpikes. Spike bursts are represented as rectangular functions from the first up to the last spike in the bursts, and with amplitude equal to the spike rate within the burst, as defined by 3.3 and 3.4

To implement this in real time, a counter initialized to 1 was maintained. Whenever a spike appeared in the train with an $ISI \leq maxISI$, the counter was incremented. Alongside, both these spikes were removed from the main train, to a temporary location. If the immediately succeeding spike also confirmed to the $ISI \leq maxISI$ criterion, the count was incremented while also transferring that new spike to the temporary location. Else, the existing contents of the temporary variable was re-populated in place into the spike train. However, if at some time, the $count \geq minSpikes$, then a burst was registered, with a burst time equal to the time stamp of the first spike in the burst train. After a burst has been detected, the removed spikes are never re-populated into the main spike train, but are cleared at the earliest possible time. This algorithm has been represented as a flow chart in Fig. 3.3.

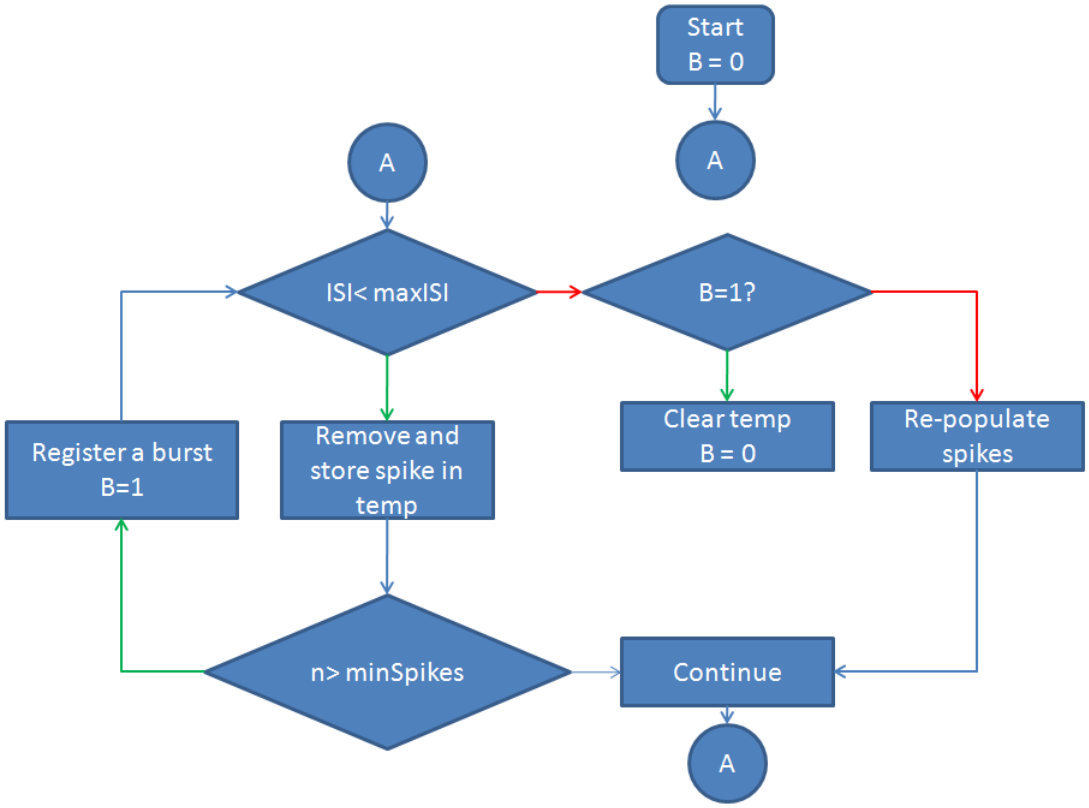

Figure 3.3: Flow chart of the real-time burst detection algorithm. B here represents a binary burst flag. The green/red connectors from a decision block correspond to the YES/NO conditions respectively.[modify slighly to show n incrementing]

3.3.3 A test bed for the real time burst detection algorithm

It was important to test the implementation of the burst detection algorithm, and the consequential segregation of the spike train into two entities: spikes outside of bursts and bursts themselves, before integrating it into the modular framework of the custom

designed interfacing software module, *HyBrain*. To this end, we developed a simple offline variant of *Hybrain* that could stream data from raw data recordings, instead of relying on data recorded from neuronal cultures and sampled by an acquisition card. In effect, the stream would simulate the data acquisition card that samples neuronal recordings at the rate of 10,000 samples/sec. The burst detection and spike train segregation strategies could be thoroughly tested and debugged on this test bed, without having to use cell cultures or the acquisition hardware. Moreover, the data processing and code optimization could be performed without the stiff timing constraints imposed by a real time implementation. This offline simplified variant was also integrated into the modular framework of the software. A screenshot of the offline variant has been included in Fig. 3.4.

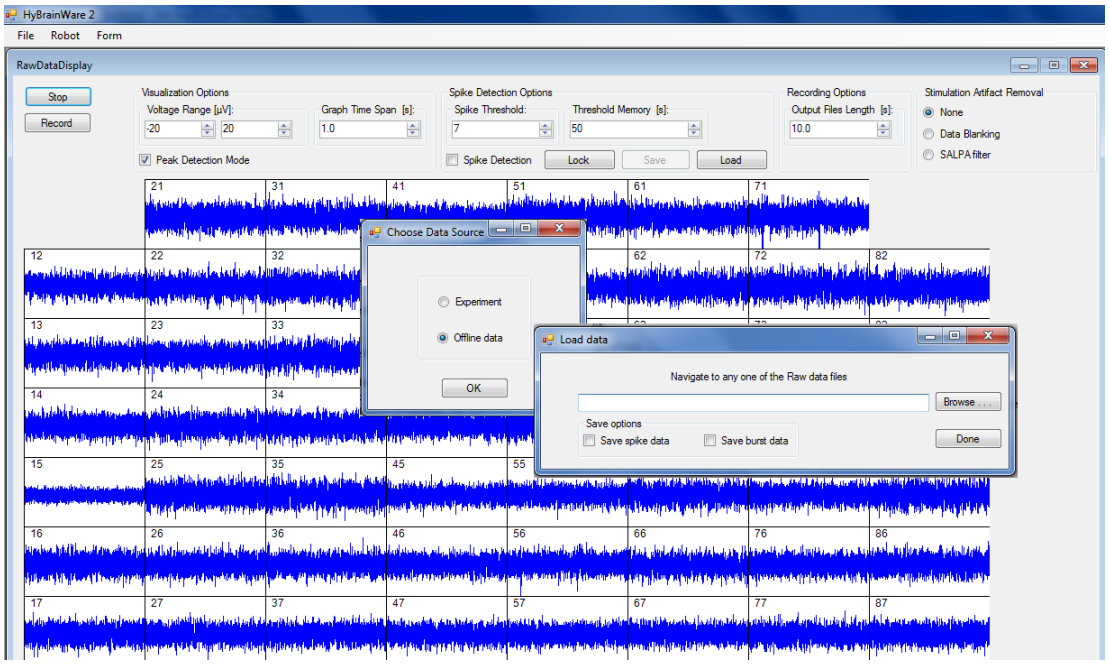

Figure 3.4: A screenshot of the offline variant of *HyBrain*.

3.4 Coding of sensory information

Sensory information coming from the external environment consists of a wide range of stimuli. According to the modern studies of Weber and Fechner on sensations psychophysics, sensory systems are able to extract four different attributes from stimuli: modality (or quality), intensity, duration and position (Kandel et al., 2000). Despite differences among them, all sensory systems share the first step, that is accomplished by specialized nervous cells, the sensory receptors: it consists in translating physical quantities (mechanical, thermal, chemical or electromagnetic energy) to which they are sensitive into a common language. Since it is known that neurons exchange information

in the form of trains of action potentials, analog, time-varying signals have to be encoded in binary signals, in order to be 'understood' by brain cells involved in memory, or decision or action. Receptor neurons converge on second order sensory neurons, located in the central nervous system. Each sensory neuron has a receptive field, composed by the receptive space from which it collects sensory information. The neuron retransmits sensory information to higher order neurons, according to a hierarchical structure. In our interface, sensory information has to be encoded into a spatio-temporal pattern of stimuli. This process is achieved by the coding block. The coding schemes we adopted were suggested by the principles described above. The coding block represents a sensory neuron, whose firing rate depends on the sensory signals it receives from the robot and affects the intensity of the feedback that reaches the neural preparation. The first step is to obtain the stimulation rate. Afterward a pulse train has to be generated that triggers the electrical stimulator. We assumed that each 'sensory neuron' of the preparation responds only to signals coming from some of the infra-red sensors, i.e. to visual stimuli affecting a limited portion of the visual field. This area can be considered as the 'receptive field' of the neuron. In our closed-loop experiments we decided to use only two stimulation sites (i.e. left and right input). Each of them should respectively be activated if the robot is approaching/hitting an obstacle by its left/right side. It is a simplified version of the most general case, in which left and right sensor activity is defined as a weighted average of, respectively, activity of left and right sensors (Cozzi, 2005). The time-varying activity of the simulated receptive fields was used to modulate the instantaneous rate of stimulation. We decided to apply a very simple neural code, i.e. a linear relationship between the overall input to the sensory neuron, computed as the weighted sum of its single inputs and its output firing rate, coinciding with the stimulation rate of the biological neurons:

$$s_{i,t} = (s_i^{MAX} - s_i^{min}) r_{i,t} + s_i^{min} \tag{3.5}$$

where subscript i denotes wheel side, $s_{i,t}$ is the stimulation rate of the i^{th} input area, and $r_{i,t}$, the sensor reading averaged over the sensors on the i^{th} side of the robot, at time sample t, whereas s_i^{MAX} and s_i^{min} are user-set parameters fixing the maximum and minimum stimulation rate.

3.5 Decoding of motor information

3.5.1 Existing scheme

The existing neuro-robotic closed loop system, developed at the Istituto Italiano di Tecnologia, Genova, is based on a simple frequency rate based algorithm (Adrian, 1928; Rieke et al., 1997). For this scheme, only a feature of the recorded signals is useful: the frequency of spikes at each location. A group of electrodes (i.e., a sub-population of neurons) on the MEA is selected and defined as the 'output area'. The number of spikes occurring over that area in a 0.1s window constitutes the basis for calculating the motor signal for the corresponding wheel. A linear relation was implemented between wheel

speed and motor signal: if no spikes are detected in a time window, the corresponding wheel turns at a set minimum speed, increasing linearly with the number of detected spikes, up to a defined maximum rate. Additionally low-pass filtering effect is added by taking into account previous samples, in order to smooth robot movements. For each wheel, the speed is therefore defined as:

$$\omega_i = \begin{cases} \frac{(f_{i,t} + f_{i,t-1})}{2f_i^{MAX}}(\omega_i^{MAX} - \omega_i^{min}) + \omega_i^{min} & \text{for } f_i < f_i^{MAX} \\ \omega_i^{MAX} & \text{for } f_i \geq f_i^{MAX} \end{cases} \tag{3.6}$$

where subscript i denotes wheel side, ω is the wheel speed and $f_{i,t}$ is the averaged firing rate over all the electrodes corresponding to the i^{th} recording area at time sample t. ω^{MAX}, ω^{min} and f^{MAX} are parameters set by the experimenter before the start of the experiment.

3.5.2 Proposed scheme

The proposed decoding scheme aims at improving the existing one by two means.

1. Consider more signal features: in particular, detect and account for bursts in the spike train

2. Introduce complexities in the functional form relating spikes/bursts to the wheel-speeds

The scheme aims at using the real time burst detection strategy to divide the main spike train into spikes outside of bursts and bursts themselves. The signature of a burst, as mentioned earlier, will be the time stamp of the first spike in that burst. The spikes outside of a burst and bursts themselves are then treated independent of each other; in effect allowing them to bear information that is distinct from one another.

The existing linear relationship between the mean firing rate and the wheel speed was replaced my a more intuitive non-linear map. Spikes (in terms of mean firing rate computed by a 100 ms window) and bursts are considered to make incremental contributions to the wheel speed in a reactive manner. An external agent (the robot in our case), may generate its actions exclusively from the available sensory information, or may use some kind of previous "experience" (Novellino et al., 2007). The former type of agent is generally referred as "reactive". Recall that the target robot behavior in this project is that of a reactive exploring vehicle paradigm, a Braitenberg vehicle. This contribution is programmed to die off at a decay rate fixed by the user.

This scheme was implemented in an iterative style, as follows. The burst contribution, was initialized to zero, i.e. $B_{i,t}\big|_{t=0} = 0$. For every 100 ms time window or equivalently 1000 sample blocks, the following operations were performed in parallel

along each of the channels selected as the right or left motor areas.

$$\begin{aligned} f_{i,t} &= 0 \\ n_{spikes}[j] &= 0 \\ \text{count } n_{spikes}[j] & \\ B_{i,t} &+= 1 \end{aligned} \tag{3.7}$$

where j is the set of channels (right or left), designated as the motor area, and $n_{spikes}[j]$ keeps a count of the number of spikes in each data block of 1000 samples, corresponding to the channels selected for the motor area. $B_{i,t}$ keeps a count of the number of bursts detected in the right or left motor areas within this datablock. At the end of each data block, the data is passed onto another part of the software where it is translated to wheelspeeds.

$$\begin{aligned} &\text{Compute the value of } f_{i,t} \\ \bar{f}_{i,t} &= \bar{f}_{i,t-1}(1-d_s) + \min(f_{i,t}, f_i^{MAX})d_s \\ B_{i,t} &= B_{i,t-1}(1-d_b) \\ D_{i,t} &= \bar{f}_{i,t}\Delta\omega_s + B_{i,t}\Delta\omega_b \\ \omega_{i,t} &= D_{i,t}(\omega_i^{MAX} - \omega_i^{min}) \\ \text{with } \bar{f}_{i,t}\big|_{t=0} &= 1 \end{aligned} \tag{3.8}$$

Following this procedure, the computation in 3.7 was repeated. As before, the subscript i denotes wheel side, $\omega_{i,t}$ is the wheel speed and $f_{i,t}$ is the averaged (spatial) firing rate over all the electrodes corresponding to the i^{th} recording area at time sample t. $\bar{f}_{i,t}$ is the weighted average with the previous value $\bar{f}_{i,t-1}$ and the minimum of $f_{i,t}$ and f_i^{MAX}; the weight being d_s, the decay rate for the spike contribution. ω^{MAX}, ω^{min} and f^{MAX} are parameters set before the start of the experiment.

Chapter 4

Closed loop experiments, results and conclusions

4.1 Introduction

In this chapter, we shall describe the experiment protocol that was followed to test the effectiveness of including bursts in decoding electrophysiological data recorded from a neuronal culture plated on a multi-electrode array. A technique to intelligently choose input-output areas or the sensory-motor areas of the culture has also been detailed. The results of the experiment and conclusions from them have also been included.

4.2 Experiment protocol

The typical experiment protocol followed consisted of a four-step procedure, each of which are described in detail.

4.2.1 Monitoring of the spontaneous activity of the culture

Before the start of the experiment session, spontaneous activity of the network is subject to observation, in order to determine, by empirical observation, which electrodes are the most likely candidate as 'input' sites (i.e. sites from which stimulation must be delivered). Typical features to look for in this phase are an adequate mean firing rate (i.e. number of spikes per second) and patterns of activity not synchronous with other regions. We developed a code in Matlab, that sorts the electrodes by a measure of their 'connection strengths' during spontaneous activity. To quantify the 'connection strengths', we computed the area under the 'conditional firing probability' of each channel within a time window. The 'conditional firing probability' $CFP(i,j)[\tau]$, may be thought of as the probability of an action potential at electrode j at time $t = tau$, given that one was detected at electrode i at $t = 0$, provided that τ belongs to the time window considered. We used Matlab for the numerical computations. The best candidates (usually a set of 8-10 strongest channels) are then selected for the second

step of the experiment.

4.2.2 Test stimulus from a set of electrodes

This step is aimed at generating the map of the effective connection (i.e. connection map) of the channels involved. It is this step that allows us to make an intelligent choice of the input-output areas(Novellino et al., 2007). In order to obtain a reactive behavior, we need the network to respond soon after the feedback stimulation, that is, we need input-output pathways characterized by a relatively early (up to 50 ms) and sustained response meaning a high strength in the functional connectivity (Shahaf and Marom, 2001). If the network reacts to the sensory feedback and the evoked electrophysiological response is characterized by a relatively long activation phase (up to 200-300 ms), the robot would not be able to react to the presence of an obstacle in 100 ms (i.e., the delay among successive serial communications between the system and the robot). This is one of the reasons why we need to accurately select the input-output pathways, beside the fact that only low-frequency stimulation can be delivered for not fatiguing the culture (Shahaf and Marom, 2001; Eytan et al., 2003).We need the stimulus-evoked response to be fast, prolonged, reliable, and therefore effective for the entire duration of the experiments.

As already said, the general aim is to have a robot that follows a specific task on the basis of the stimulated electrophysiological activity shown by the neuronal culture. To this end, it is a fundamental prerequisite to characterize the collective activity of the network that will be connected to the robot (i.e., analysis of both spontaneous and stimulus evoked neuronal activity). This characterization phase is necessary since the unstructured nature of the culture does not allow us to a priori define the sensory and motor areas that will be connected with the sensory and motor areas of the robot, as it happens with portion of tissue with a well-defined sensorimotor architecture (Reger et al., 2000; Karniel et al., 2005).

Thus, the goal of the characterization phase is to select those channels of the MEA to be used as sensory inputs (i.e., connected to the robots sensors) and motor outputs (i.e., connected to the robots wheels) of the biological network. To test the response to stimulation from different sites in different areas of the neuronal network, trains of 50 electrical stimuli are delivered (1.5V peak to peak-extracellular stimulation, 500 s, and duty cycle 50%). This procedure is repeated from at least 5 arbitrarily chosen micro-electrodes (Wagenaar and Potter, 2004). The poststimulus time histogram-(PSTH) (i.e., the average number of spikes obtained in response to a stimulus, at different latencies) is then used for quantifying the strength of connections between a specific stimulating sites and all the other recording sites. It is the impulse response (in terms of instantaneous firing rate) to a single test stimulus. A typical PSTH has been shown in fig. 4.1.

The algorithm for the selection of the output (motor) and input (sensory) sites supplies the I/O pairs corresponding to maximum selectivity and it is based on network effective functional interconnectivity. The ideal case is described in the following: given two (or more) stimulating channels (e.g., S1 and S2) and two groups of recording sites (e.g., R1 and R2), the strength of the connectivity S1-R1 and S2-R2 is “high” and

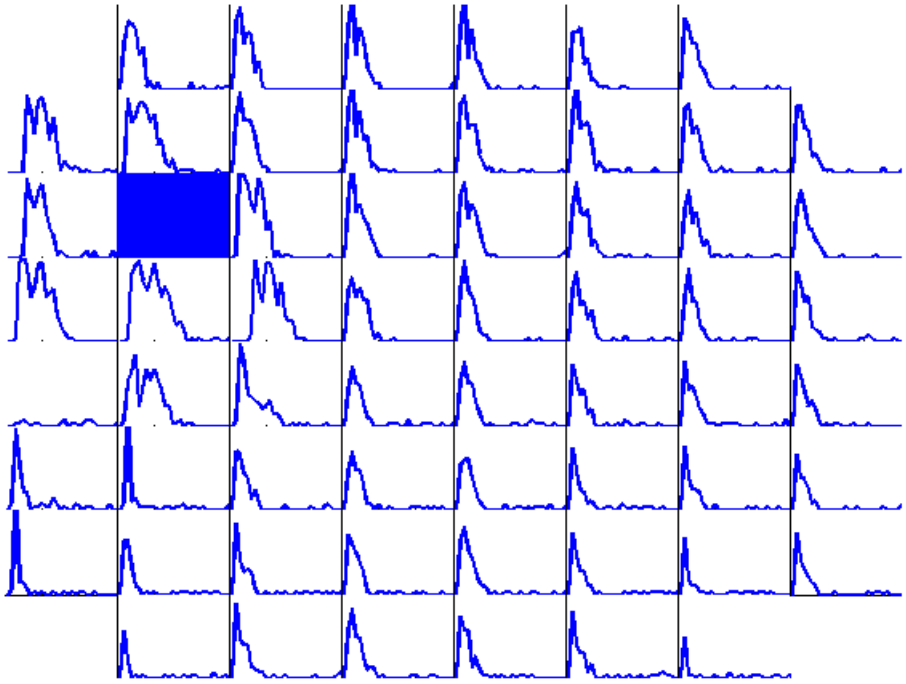

Figure 4.1: A typical PSTH of evoked responses in a neuronal network. The solid filled channel was the one used for stimulation.

simultaneously, the strength of the connectivity S1-R2, and S2-R1 is "low" (i.e., good selectivity in input-output pairs). The described scheme guarantees to a certain degree, that the responses in the two (groups of) recording sites are different on the basis of the stimulating electrodes. Of course the above is an ideal situation and, since the mean connectivity of the network is high, also due to the high density of plated cells, it is hard to get highly specific responses in the input-output pathways.

The methodology that we used to make a selection of the pathways is the "selectivity map" or "connectivity map" (see fig. 4.2). Each dot represents the PSTH area at a specific recording site given that there was a stimulation from a couple of stimulating sites. All the possible input-output combinations are explored and only the pathways producing responses lying more distant from the diagonal (i.e., closer to the axis) are selected. Those specific pathways (of sensory-motor activations) can be then conveniently utilized for driving the robot and for implementing simple reactive behaviors (e.g. obstacle avoidance).

4.2.3 Random- turn experiments

The next step involved running a set of four 20-minute long "Random-turn experiments". A "Random-turn experiment" involved three arenas: one with a straight path, another with with a right turn, and the last one with a left turn. The turns are smooth and resemble a section of a two dimensional annulus. Each arena has only the ends of the annular segment as the exit points. The walls serve as the only obstacles that the robot sees (see fig. 4.3). The robot is initially positioned at the center of one of the exits of

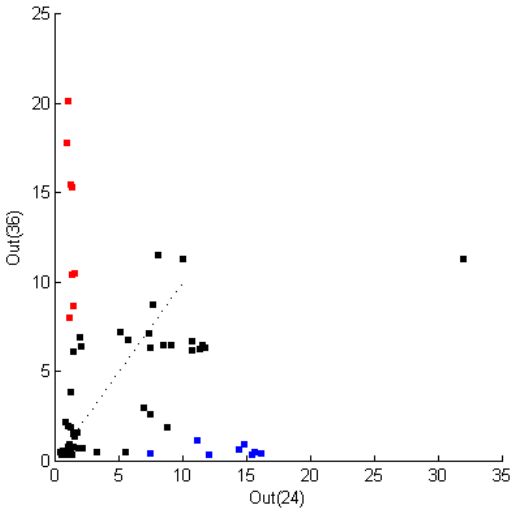

Figure 4.2: A typical connectivity map. It represents a plot of the PSTH areas evoked by a couple of stimulating electrodes on a specific electrode.

the arena. It is expected to navigate out of the arena through the opposite exit, for the run to be counted as a 'successful' one. As soon as the robot exits through one of the two open ends, it is presented with a new arena. The choice of arena is randomly made from the above mentioned set of three possible arenas.

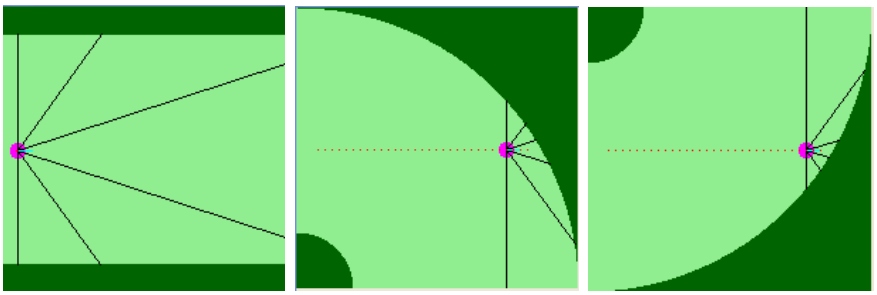

(a) Straight path **(b)** Right turn **(c)** Left turn

Figure 4.3: Arenas of the random turn experiments. The pink circle is the virtual robot. The six lines around the robot is a visualization of the distance to the wall (the obstacle) as measured from the six sensors on the robot.

Each of the four robot runs performed had a different increment in wheel speed due to the presence of spikes or bursts. The first run depended solely on spikes and ignored bursts. The second and third runs had both spikes and bursts influencing the wheel speeds; but one being more dominant than the other in each of these cases respectively. The final run had both spikes and bursts exerting equal influence in robot wheel speed increments.

4.2.4 Spontaneous activity and connection map

We finished by monitoring the spontaneous activity of the culture once again for a 10 min period. A connection map was also generated by stimulating the same electrodes as in §4.2.2. The idea was to gather data in order to monitor changes in activity patterns or connection strengths between channel pairs as a result of the robot runs that the culture was exposed to. The analysis itself was however beyond the scope of this particular thesis work.

4.3 Indicators of robot performance

Before we present the results, we define the framework within which the results were evaluated. The two parameters that we selected to evaluate the performance of the neurorobotic system were

(i) Rate of successful trials (see §4.2.3 for the definition of a 'successful' robot run)

(ii) Time required for robot exit

The tools for the offline data processing aimed at the analysis of the behavior of the neurorobotic system were developed using Matlab.

4.4 Results

Fig. 4.4 shows the success rates of the robot runs averaged over all experiments conducted. A total of ten experiments were considered in the evaluation of these results. The x-axis represents the four different robot runs. The 'H' in the x-axis label stands for 'high', and corresponds to an increment in wheel speed, $\Delta\omega$ of 0.1. The 'L1' stands for 'Low-1' and corresponds to a $\Delta\omega$ of 0, while 'L2' or 'Low-2' corresponds to a $\Delta\omega$ of 0.05. The 'S' and 'B' in the labels stand for 'spikes' and 'bursts' respectively. Therefore the labels corresponding to each of the four sets of robot runs may be summarized as follows.

(i) HSL1B: $\Delta\omega_s = 0.1$ and $\Delta\omega_b = 0$

(ii) HSL2B: $\Delta\omega_s = 0.1$ and $\Delta\omega_b = 0.05$

(iii) L2SHB: $\Delta\omega_s = 0.05$ and $\Delta\omega_b = 0.1$

(iv) L2SL2B: $\Delta\omega_s = 0.05$ and $\Delta\omega_b = 0.05$

The decay rates of both the spikes and bursts were fixed at a constant value, for each set of robot runs.

$$d_s = d_b = 0.1$$

Fig. 4.6 shows the time taken for each trial to be completed.

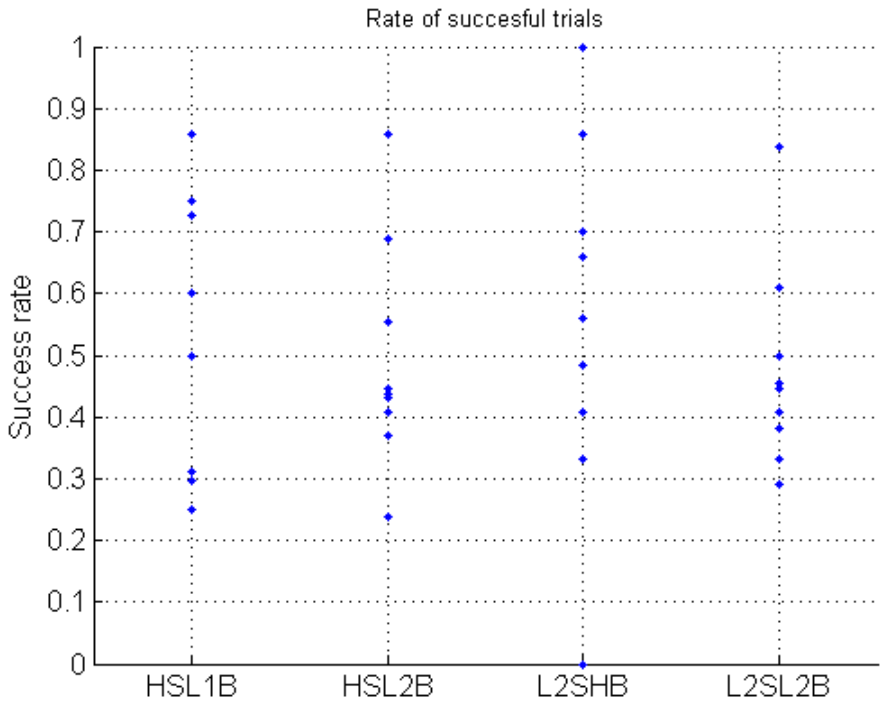

Figure 4.4: Plot of the success rates of the robot. The x-axis represents the four sets of robot runs.

4.5 Discussion

From the plots of chosen indicators of robot performance, it appears that the modified decoding scheme has no significant impact on the performance of the robot. The median success rate in all cases lies very close to 0.5. However, cases HSL2B and L2SHB, seem interesting. Recall that these cases correspond to high and low contributions from spikes and bursts respectively, in case: HSL2B and exactly the opposite in case:L2SHB. From the figure of success rate, fig. 4.5, it seems that letting bursts contribute more, was improving the success rates. Observing these cases in fig. 4.7 also suggests that letting the bursts contribute more was slightly adding to the mean robot speeds. A combination of greater robot speeds and higher success rates could only imply added navigation capabilities. However, it is not clear why the success rates of case: HSL1B, where the contribution to wheel speeds was entirely from spikes and not at all from bursts, is not achieved by another cases.

There are many possible explanations for the observations made from these experiments, each of which needs careful re-evaluation. We shall state them in the form of open questions.

i. Was the design of the experiment insufficient to manifest the differences in the signal features as captures by the decoding scheme?

ii. Were the parameters used for in the decoding scheme (decay rates as well as con-

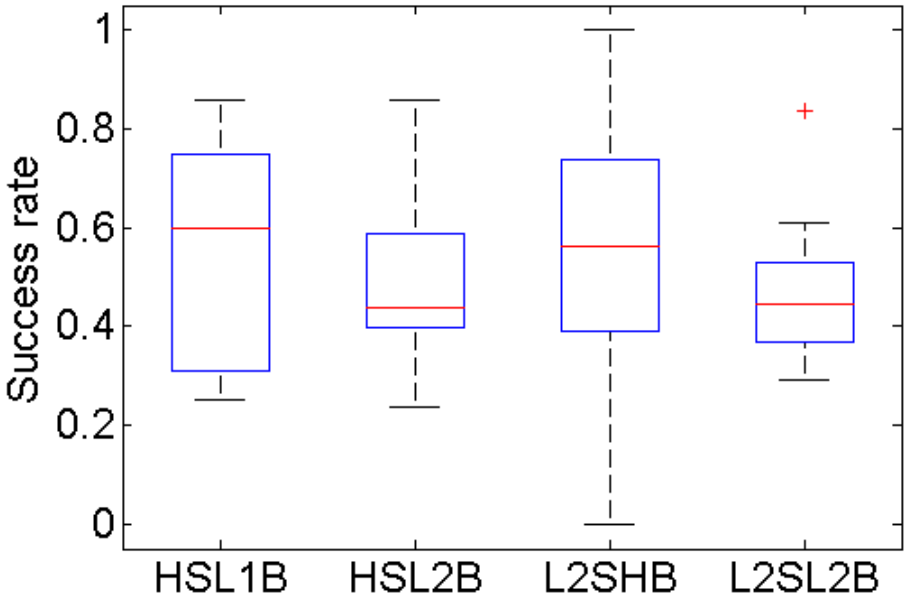

Figure 4.5: Boxplot of the success rates of the robot. The x-axis represents the four sets of robot runs.

tributions to wheel speeds) optimal? Would tuning them lead to better results?

iii. Was the choice of motor areas sufficient to gather information about the bursts from the neuronal network? This particular question was motivated by the fact that the motor areas for our experiments, were chosen only on the basis of post stimulus spiking response. While quantifying the parameters that characterized the culture, (namely, 'connectivity' and 'selectivity'), the bursting behavior was not accounted for. It was an unstated assumption that greater the spiking activity implied greater bursting activity. However, preliminary data analysis, we performed on the post stimulus network behavior for some of the cultures, seem to refute this assumption. The fig. 4.8 shows the mean of the burst counts in each of the channels, during 4.5 seconds, following each of the 30 stimulations presented at the selected input sites for that particular culture. The red stars in some of the channels mark those that were selected for the motor areas. The top and bottom sub-figures correspond to stimulation presented at the left and right input sites respectively. A similar observation was also made for the spike counts following stimulation. The resulting bar graph has been plotted in fig. 4.9. As can be observed, the while the peak of the evoked spike count corresponds to channel 39 for stimulation at both left and right input areas, the peak for the burst activity was channel 52 and 49 for stimulation presented at the left and right input areas respectively.

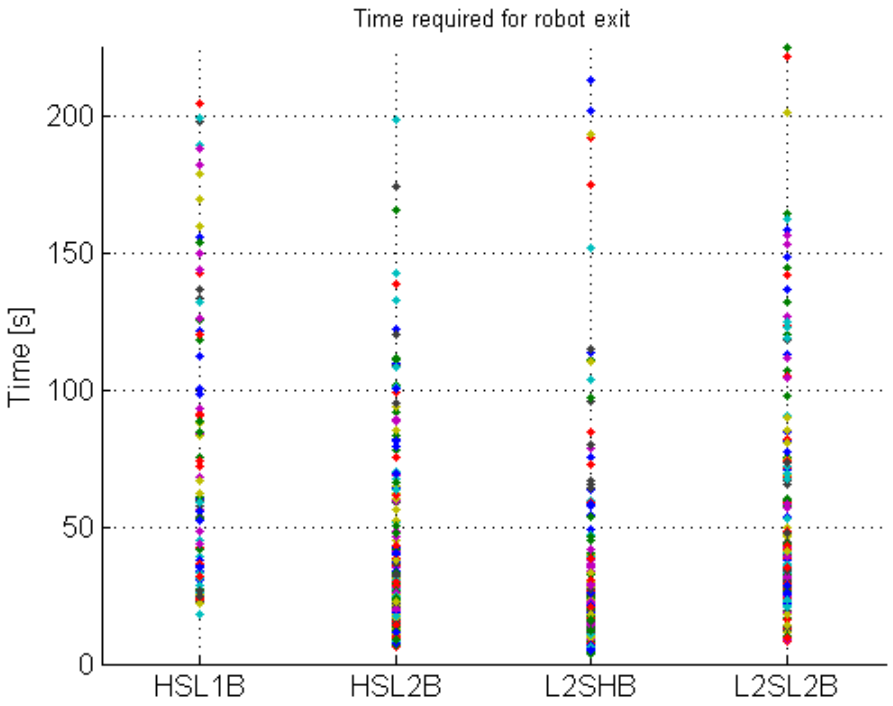

Figure 4.6: Plot of the different times the robot took to exit the arena. Each color represents a different robot run. The data of all experiments have been pooled together. The x-axis represents the four sets of robot runs.

4.6 Conclusions and future directions

The aim of the thesis i.e. to develop a software framework to consider an additional signal feature and use it in a new decoding scheme, was achieved. The new scheme was tested using closed loop neuro-robotic experiments. Basic data analysis of the results obtained has been presented.

The implemented framework could serve as a basis for a more refined investigation into both better decoding schemes as well better understanding the role that bursting behavior plays. It was observed during the course of experiments that bursting behavior in hippocampal cultures differed from that of cortical cultures. Differences in performance of the robot (with the augmented scheme) between cortical and hippocampal cultures need to be evaluated more closely. The differences in robot performance between confined and random cultures could also be an interesting point to be investigated.

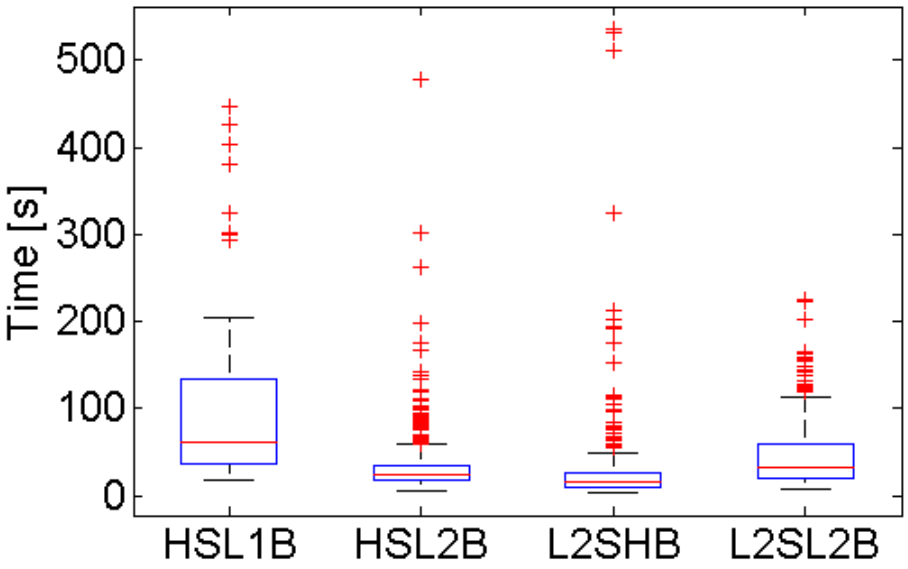

Figure 4.7: Plot of the different times the robot took to exit the arena. Each color represents a different robot run. The data of all experiments have been pooled together. The x-axis represents the four sets of robot runs.

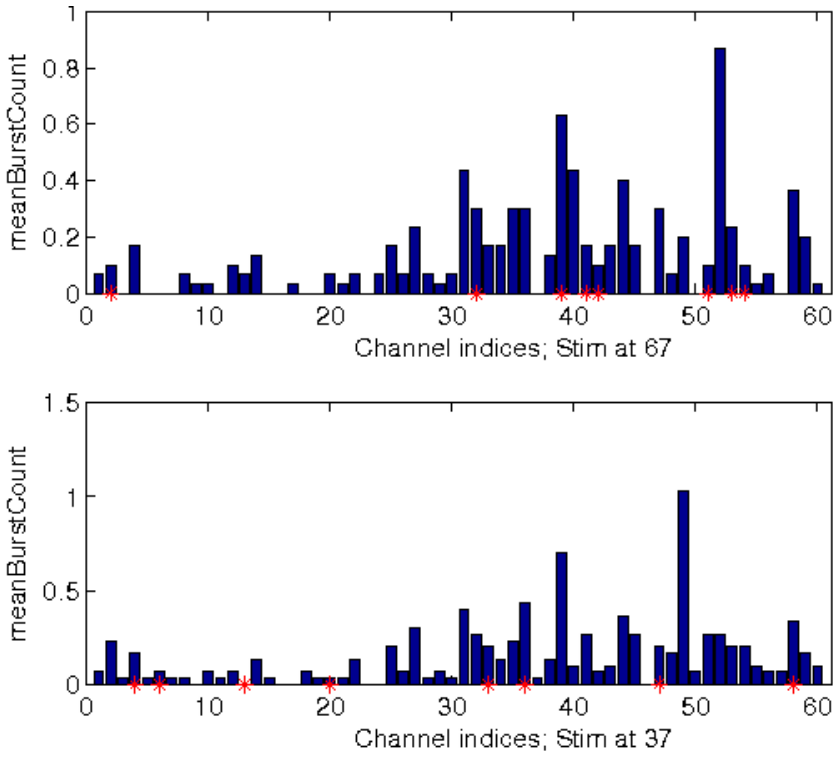

Figure 4.8: Plot of the mean burst count in each channel following stimulation at the left (top sub graph) and right (bottom subgraph) input areas.

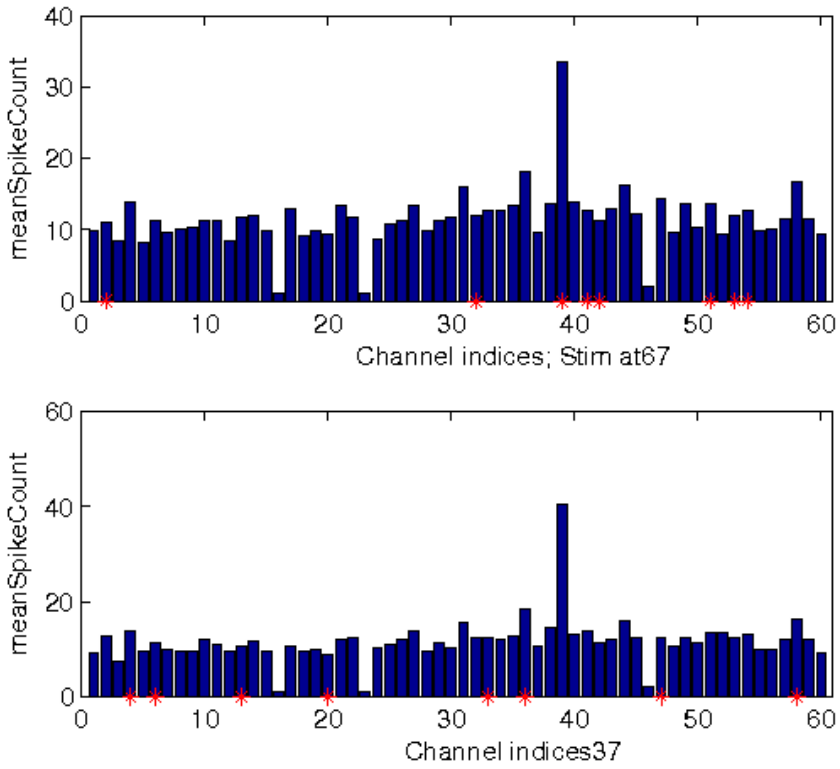

Figure 4.9: Plot of the mean spike count in each channel following stimulation at the left (top sub graph) and right (bottom subgraph) input areas.

Bibliography

Adrian, E. D. (1928). *The basis of sensation: the action of sense organs*. W. W. Norton & C., New York, USA.

Araque, A., Parpura, V., Sanzgiri, R. P., and Haydon, P. G. (1999). Tripartite synapses: glia, the unacknowledged partner. *Trends Neurosci.*, 22(5):208–215.

Augusti-Tocco, G. and Sato, G. (1969). Establishment of functional clonal lines of neurons from mouse neuroblastoma. *Proc Natl Acad Sci U S A*, 64(5):311–315.

Bakkum, D., Shkolnik, A., Ben-Ari, G., Gamblen, P., De Marse, T., and Potter, S. (2004). Removing some 'a' from ai: Embodied cultured networks. In Iida, F., Pfeifer, R., Steels, L., and Kuniyoshi, Y., editors, *Embodied Artificial Intelligence*, volume 3139 of *Lecture Notes in Computer Science*, pages 130–145. Springer.

Banker, G. and Goslin, K. (1998). *Culturing Nerve cells*. MIT Press.

Beggs, J. and Plenz, D. (2003). Neuronal avalanches in neocortical circuits. *J Neurosci.*, 23(35):11167–11177.

Berdondini, L., Imfeld, K., Maccione, A., Tedesco, M., Neukom, S., Koudelka-Hep, M., and Martinoia, S. (2009). Active pixel sensor array for high spatio-temporal resolution electrophysiological recordings from single cell to large scale neuronal networks. *Lab Chip*, 9:2644–2651.

Blau, A., Neumann, T., Ziegler, C., and Benfenati, F. (2009). Replicamoulded polydimethylsiloxane culture vessel lids attenuate osmotic drift in long-term cell cultures. *J Biosci*, 34(1):59–69.

Braitenberg, V. (1984). *Vehicles - Experiments in synthetic psychology*. The MIT Press, Cambridge (MA, USA).

Bray, D. (1970). Surface movements during the growth of single explanted neurons. *Proc Natl Acad Sci U S A*, 65:905–910.

Brewer, G. (1997). Isolation and culture of adult rat hippocampal neurons. *J. Neurosci Methods*, 71(2):143–155.

Brewer, G., Boehler, M., Ide, A., and Wheeler, B. (2009a). Chronic electrical stimulation of cultured hippocampal networks increases spontaneous spike rates. *J Neurosci Methods*, 184(1):104–109.

Brewer, G., Boehler, M., Pearson, R., DeMaris, A., Ide, A., and Wheeler, B. (2009b). Neuron network activity scales exponentially with synapse density. *J Neural Eng*, 6(1):014001.

Brewer, G., Torricelli, J., Evege, E., , and Price, P. (1993). Optimized survival of hippocampal neurons in b27-supplemented neurobasal, a new serum-free medium combination. *J. Neurosci Res*, 35(5):567–576.

Carrell, A. and Burroughs, M. (1910). Cultivation of adult tissues and organs outside of the body. *JAMA*, 55:1379–1381.

Chiappalone, M., Bovea, M., Vato, A., Tedesco, M., and Martinoia, S. (2006). Dissociated cortical networks show spontaneously correlated activity patterns during in vitro development. *Brain Res*, 1093(1):41–53.

Chiappalone, M., Massobrio, P., and Martinoia, S. (2008). Network plasticity in cortical assemblies. *Eur J Neurosci*, 28(1):221–237.

Chiappalone, M., Novellino, A., Vajda, I., Vato, A., Martinoia, S., and Van Pelt, J. (2005). Burst detection algorithms for the analysis of spatio-temporal patterns in cortical networks of neurons. *Neurocomputing*, 65:653–662.

Chien, C. and Pine, J. (1991). Voltage sensitive dye recording of action potentials and synaptic potentials from sympathetic microcultures. *BiophysJ*, 60:697–711.

Cozzi, L. (2005). *Bi-Directional neural interfaces: Design, implementation and investigation of Neural coding*. PhD thesis, University of Genova.

Cozzi, L., D'Angelo, P., Chiappalone, M., Ide, A., Novellino, A., Martinoia, S., and Sanguineti, V. (2005). Coding and decoding of information in a bi-directional neural interface. *Neurocomputing*, 65-66:783–792.

Crain, S. (1976). *Neurophysiological studies in tissue culture.* Raven Press.

De Simoni, A. and Yu, L. (2006). Preparation of organotypic hippocampal slice cultures: interface method. *Nat Protoc*, 3:1439–1445.

DeMarse, T., Wagenaar, D., Blau, A., and Potter, S. (2001). The neurally controlled animat: biological brains acting with simulated bodies. *Auton Robots*, 11:305–310.

Doiron, B., Chacron, M., Maler, L., Longtin, A., and Bastian, J. (2003). Inhibitory feedback required for network oscillatory responses to communication but not prey stimuli. *Nature*, 421:539–543.

Egert, U., Schlosshauer, B., Fennrich, S., Nisch, W., Fejtl, M., Knott, T., Muller, T., and Hammerle, H. (1998). A novel organotypic long-term culture of the rat hippocampus on substrate-integrated multielectrode arrays. *Brain Res Brain Res Protoc*, 2(4):229–242.

Elshabini-Riad, A. and Barlow, F. (1998). *Thin Film Technology Handbook*. McGraw-Hill, New York, USA.

Eytan, D., Brenner, N., and Marom, S. (2003). Selective adaptation in networks of cortical neurons. *Journal of Neuroscience*, 23(28):9349–56.

Eytan, D. and Marom, S. (2006). Dynamics and effective topology underlying synchronization in networks of cortical neurons. *J Neurosci*, 26(33):8465–8476.

Fejtl, M., Stett, A., Nisch, W., Boven, K.-H., and Möller, A. (2006). On micro-electrode array revival: Its development, sophistication of recording, and stimulation. In (Taketani and Baudry, 2006).

Fellin, T. (2009). Communication between neurons and astrocytes: relevance to the modulation of synaptic and network activity. *J Neurochem*, 108:533–544.

Frey, U., Egert, U., Heer, F., Hafizovic, S., and Hierlemann, A. (2009). Microelectronic system for high-resolution mapping of extracellular electric fields applied to brain slices. *Biosens Bioelectron*, 24:2191–2198.

Fromherz, P., Offenhausser, A., Vetter, T., and Weis, J. (1991). A neuronsilicon junction: A retzius cell of the leech on an insulated-gate field effect transistor. *Science*, 252:1290–1293.

Fromherz, P. and Stett, A. (1995). Silicon-neuron junction: Capacitive stimulation of an individual neuron on a silicon chip. *Phys Rev Lett*, 75:1670–1673.

Gabbiani, F., Metzner, W., Wessel, R., and C., K. (1996). From stimulus encoding to feature extraction in weakly electric fish. *Nature*, 384(6609):564–567.

Gähwiler, B. (1981). Organotypic monolayer cultures of nervous tissue. *Neurosci Methods*, 4:329–342.

Gramowski, A., Jugelt, K., Weiss, D., and Gross, G. (2004). Substance identification by quantitative characterization of oscillatory activity in murine spinal cord networks on microelectrode arrays. *Eur J Neurosci,*, 19(10):2815–2825.

Gramowski, A., Schiffmann, D., and Gross, G. W. (2000). Quantification of acute neurotoxic effects of trimethyltin using neuronal networks cultured on microelectrode arrays. *Neurotoxicology*, 21(3):331–342.

Gross, G. (1994). Internal dynamics of randomized mammalian networks in culture. In (Stenger and McKenna, 1994), pages 277–317.

Gross, G., Azzazy, H., Wu, M., and Rhodes, B. (1995). The use of neuronal networks on multielectrode arrays as biosensors. *Biosens Bioelectron*, 10:553–567.

Gross, G., Reiske, E., Kreutzberg, G., and Mayer, A. (1977). A new fixed-array multi-microelectrode system designed for long-term recording of extracellular single unit activity in vitro. *Neurosci Lett*, 6:101–105.

Gross, G., Rhoades, B., and Jordan, R. (1992). Neuronal networks for biochemical sensing. *Sens Actuators*, 6:1–8.

Gross, G. W., Williams, A. N., and Lucas, J. H. (1982). Recording of spontaneous activity with photoetched microelectrode surfaces from mouse spinal neurons in culture. *J Neurosci Methods*, 5(1-2):13–22.

Harrison, R. (1907). Observations on the living developing nerve fiber. *Anat Rec*, 1:116–118.

Harrison, R. (1912). The cultivation of tissues in extraneous media as a method of morphogenetic study. *Anat Rec*, 6:181–193.

Imfeld, K., Neukom, S., Maccione, A., Bornat, Y., Martinoia, S., Farine, P., Koudelka-Hep, M., and Berdondini, L. (2008). Large-scale, high resolution data acquisition system for extracellular recording of electrophysiological activity. *IEEE Trans Biomed Eng*, 55(8):2067–73.

Izhikevich, E., Desai, N., Walcott, E., and Hoppensteadt, F. (2003). Bursts as a unit of neural information: selective communication via resonance. *Trends in Neuroscience*, 26:161–167.

Jahnsen, H., Kristensen, B. W., Thièbaud, P., Noraberg, J., Jakobsen, B., Bove, M., Martinoia, S., Koudelka-Hep, M., Grattarola, M., and Zimmer, J. (1999). Coupling of organotypic brain slice cultures to silicon-based arrays of electrodes. *Methods*, 18(2):160 –172.

Jimbo, Y., Kawana, A., Parodi, P., and Torre, V. (2000). The dynamics of a neuronal culture of dissociated cortical neurons of neonatal rats. *Biological Cybernetics*, 83:1–20.

Jimbo, Y., Tateno, Y., and Robinson, H. (1999). Simultaneous induction of pathway-specific potentiation and depression in networks of cortical neurons. *Biophys J*, 76:670–678.

Jobling, D., Smith, J., and Wheal, H. (1981). Active microelectrode array to record from the mammalian central nervous system *in vitro*. *Med Biol. Eng. Comp,*, 19:553–560.

Kamioka, H., Jimbo, Y., Charlety, P., and Kawana, A. (1997). Planar electrode arrays for long-term measurement of neuronal firing in cultured cortical slices. *Cellular Eng*, 2:148–153.

Kandel, E. R., Schwartz, J. H., and Jessell, T. M. (2000). *Principles of Neural Science*. McGraw-Hill Medical, 4th edition.

Karniel, A., Kositsky, M., and Fleming, K. (2005). Computational analysis in vitro: dynamics and plasticity of a neuro-robotic system. *Journal of Neural Engineering*, 2(3):S250 – S265.

Keefer, E., Gramowski, A., Stenger, D., Pancrazio, J., and Gross, G. (2001). Characterization of acute neurotoxic effects of trimethylolpropane phosphate via neuronal network biosensors. *Biosens Bioelectron*, 16:513–525.

Kettenmann, H. and Grantyn, R. (1992). *Practical electrophysiological methods: a guide for in vitro studies in vertebrate neurobiology*. Number p. 895 in Practical Electrophysiological Methods: A Guide for in Vitro Studies in Vertebrate Neurobiology. Wiley-Liss.

Lesica, N. and Stanley, G. (2004). Encoding of natural scene movies by tonic and burst spikes in the lateral geniculate nucleus. *J. Neurosci.*, 24:10731–10740.

Lisman, J. (1997). Bursts as a unit of neural information: making unreliable synapses reliable. *, Trends in Neuroscience*, 20:38–43.

Maccione, A., Gandolfo, M., Massobrio, P., Novellino, A., Martinoia, S., and Chiappalone, M. (2009). A novel algorithm for precise identification of spikes in extracellularly recorded neuronal signals. *Journal of Neuroscience Methods*, 177(1):241 – 249.

Maeda, E., Robinson, H., and Kawana, A. (1995). The mechanisms of generation and propagation of synchronized bursting in developing networks of cortical neurons. *The Journal of Neuroscience*, 15(10):6834–6845.

Maher, M., Pine, J., Wright, J., and Tai, Y.-C. (1999). The neurochip: a new multi-electrode device for stimulating and recording from cultured neurons. *Journal of Neuroscience Methods*, 87(1):45 – 56.

Martinoia, S., Bonzano, L., Chiappalone, M., and Tedesco, M. (2005a). Electrophysiological activity modulation by chemical stimulation in networks of cortical neurons coupled to microelectrode arrays: A biosensor for neuropharmacological applications. *Sensors and Actuators B: Chemical*, 108(12):589 – 596.

Martinoia, S., Bonzano, L., Chiappalone, M., Tedesco, M., Marcoli, M., and Maura, G. (2005b). In vitro cortical neuronal networks as a new high-sensitive system for biosensing applications. *Biosensors and Bioelectronics*, 20(10):2071 – 2078.

Martinoia, S., Massobrio, P., Bove, M., and Massobrio, G. (2004a). Cultured neurons coupled to microelectrode arrays: circuit models, simulations and experimental data. *IEEE Transactions on Bio-medical Engineering*, 51(5):859–864.

Martinoia, S., Sanguineti, V., Cozzi, L., Berdondini, L., van Pelt, J., Tomas, J., Masson, G. L., and Davide, F. (2004b). Towards an embodied in vitro electrophysiology: the neurobit project. *Neurocomputing*, 5860(0):1065 – 1072.

MATLAB (2009). *version 7.9.0 (R2009b)*. The MathWorks Inc., Natick, Massachusetts.

Meister, M., Pine, J., and Baylor, D. (1989). Multielectrode recording from the vertebrate retina. *Invest Ophthalmol Vis Sci*, 30 (Suppl.)(68):859–864.

Meister, M., Pine, J., and Baylor, D. (1994). Multi-neuronal signals from the retina: acquisition and analysis. *Journal of Neuroscience Methods*, 51:95–106.

Mulas, M., Massobrio, P., Martinoia, S., and Chiappalone, M. (2010). A simulated neuro-robotic environment for bi-directional closed-loop experiments. *Paladyn. Journal of Behavioral Robotics*, 1:179–186. 10.2478/s13230-011-0004-x.

Mussa-Ivaldi, S., Alford, S. T., Chiappalone, M., Fadiga, L., Karniel, A., Kositsky, M., Maggiolini, E., Panzeri, S., Sanguineti, V., Semprini, M., and Vato, A. (2010). New perspectives on the dialogue between brains and machines. *Frontiers in Neuroscience*, 3(8).

Nedergaard, M. (1994). Direct signaling from astrocytes to neurons in cultures of mammalian brain cells. *Science*, 263(5154):1768–71.

Noraberg, J., Kristensen, B., and Zimmer, J. (1999). Markers for neuronal degeneration in organotypic slice cultures. *Brain Res Brain Res Protoc*, 3:278–290.

Novellino, A., D'Angelo, P., Cozzi, L., Chiappalone, M., Sanguineti, V., and Martinoia, S. (2007). Connecting neurons to a mobile robot: An in vitro bidirectional neural interface. *Comput Intell Neurosci.*, 33:1204–12.

Oka, H., Shimono, K., Ogawa, R., Sugihara, H., and Taketani, M. (1999). A new planar multielectrode array for extracellular recording: application to hippocampal acute slice. *Journal of Neuroscience Methods*, 93(1):61 – 67.

Oswald, A., Chacron, M., Doiron, B., Bastian, J., and Maler, L. (2004). Parallel processing of sensory input by bursts and isolated spikes. *J Neurosci.*, 24(18):4351–62.

Pasquale, V. (2009). *Analysis of the network dynamics of cultured neurons coupled to microelectrode arrays: from spontaneous to evoked activity patterns*. PhD thesis, Italian Institute of Technology and University of Genova.

Pasquale, V., Massobrio, P., Bologna, L., Chiappalone, M., and Martinoia, S. (2008). Self-organization and neuronal avalanches in networks of dissociated cortical neurons. *Neuroscience*, 153(4):1354 – 1369.

Perkel, D. (1967). Neuronal spike train and stochastic point processes i. the single spike train. *Biophys. J.*, 7:391–418.

Pfrieger, F. W. and Barres, B. A. (1997). Synaptic efficacy enhanced by glial cells in vitro. *Science*, 277(5332):1684–87.

Pine, J. (1980). Recording action potentials from cultured neurons with extracellular microcircuit electrodes. *J Neurosci Methods*, 2(1):19–31.

Pine, J. (2006). A history of mea development. In (Taketani and Baudry, 2006).

Raichman, N. and Ben-Jacob, E. (2008). Identifying repeating motifs in the activation of synchronized bursts in cultured neuronal networks. *J Neurosci Methods*, 170(1):96–110.

Regehr, W., Pine, J., Cohan, C., Mischke, M., and Tank, D. (1989). Sealing cultured neurons to embedded dish electrodes facilitates long-term stimulation and recording. *J Neurosci Methods*, 30:91–106.

Reger, B. D., Fleming, K. M., Sanguineti, V., Alford, S., and Mussa-Ivaldi, F. A. (2000). Connecting brains to robots: An artificial body for studying computational properties of neural tissues. *Artificial Life*, pages 307–324.

Reinagel, P., Godwin, D., Sherman, S., and C., K. (1999). Encoding of visual information by lgn bursts. *J Neurophysiol.*, 81:2558–69.

Rieke, F., Warland, D., Steveninck, R., and Bialek, W. (1997). *Spikes: exploring the neural code*. The MIT Press, Cambridge (MA, USA).

Robinson, D. (1968). The electrical properties of metal microelectrodes. *Proc. IEEE*, 56:1065–1071.

Shahaf, G. and Marom, S. (2001). Learning in networks of cortical neurons. *J Neurosci*, 21:8782–8788.

Sherman, S. (2001). Tonic and burst firing: dual modes of thalamocortical relay. *Trends in Neuroscience*, 24:122–126.

Shimono, K., Brucher, F., Granger, R., Lynch, G., and Taketani, M. (2000). Origins and distribution of cholinergically induced rhythms in hippocampal slices. *The Journal of Neuroscience*, 20(22):8462–8473.

Stenger, D. and McKenna, T., editors (1994). *Enabling Technologies for Cultured Neural Networks*, Lecture Notes in Computer Science, New York, USA. Academic Press.

Stett, A., Barth, W., Weiss, S., Haemmerle, H., and Zrenner, E. (2000). Electrical multisite stimulation of the isolated chicken retina. *Vision Res*, 40:1785–1795.

Stoppini, L., Buchs, P.-A., and Muller, D. (1991). A simple method for organotypic cultures of nervous tissue. *Journal of Neuroscience Methods*, 37(2):173 – 182.

Taketani, M. and Baudry, M., editors (2006). *Advances in Network Electrophysiology Using Micro-Electrode Arrays*, New York, USA. Springer-Science.

Tam, D. and Gross, G. (1994). Extraction of dynamical changes in neuronal network circuitries using multiunit spike train analysis. In (Stenger and McKenna, 1994).

Tam, D. C. (2002). An alternate burst analysis for detecting intra-burst firings based on inter-burst periods. *Neurocomputing*, 4446(0):1155 – 1159.

Tehovnik, E. J. (1996). Electrical stimulation of neural tissue to evoke behavioral responses. *Journal of Neuroscience Methods*, 65(1):1 – 17.

Thomas, Jr, C., Springer, P., Loeb, G., Berwald-Netter, Y., and Okun, L. (1972). A miniature microelectrode array to monitor the bioelectric activity of cultured cells. *Experimental Cell Research*, 74(1):61 – 66.

van Pelt, J., Corner, M., Wolters, P., Rutten, W., and Ramakers, G. (2004). Longterm stability and developmental changes in spontaneous network burst firing patterns in dissociated rat cerebral cortex cell cultures on multielectrode arrays. *Neuroscience Letters*, 361(1-3):86–89.

Wagenaar, D., Madhavan, R., Pine, J., and Potter, S. (2005). Controlling bursting in cortical cultures with closed-loop multi-electrode stimulation. *J Neurosci.*, 25:680–688.

Wagenaar, D., Pine, J., and Potter, S. (2006). An extremely rich repertoire of bursting patterns during the development of cortical cultures. *BMC Neurosci*, 7(11).

Wagenaar, D. A. and Potter, S. M. (2004). A versatile all-channel stimulator for electrode arrays, with real-time control. *Journal of Neural Engineering*, 1(1):39.

Wheeler, B. and Novak, J. (1986). Current source density estimation unsing microelectrode array data from the hippocampal slice preparation. *IEEE Trans Biomed Eng*, 33:1204–12.

Whitson, J., Kubota, D., Shimono, K., Jia, Y., and Taketani, M. (2006). Multi-electrode arrays: Enhancing traditional methods and enabling network physiology. In (Taketani and Baudry, 2006).

Zernike, F. (1934). Beugungstheorie des schneidenverfahrens und seiner verbesserten form, der phasenkontrastmethode. *Physica*, 1:689–704.